2023 2nd Season Stock Assessment

Falkland calamari

(*Doryteuthis gahi*)

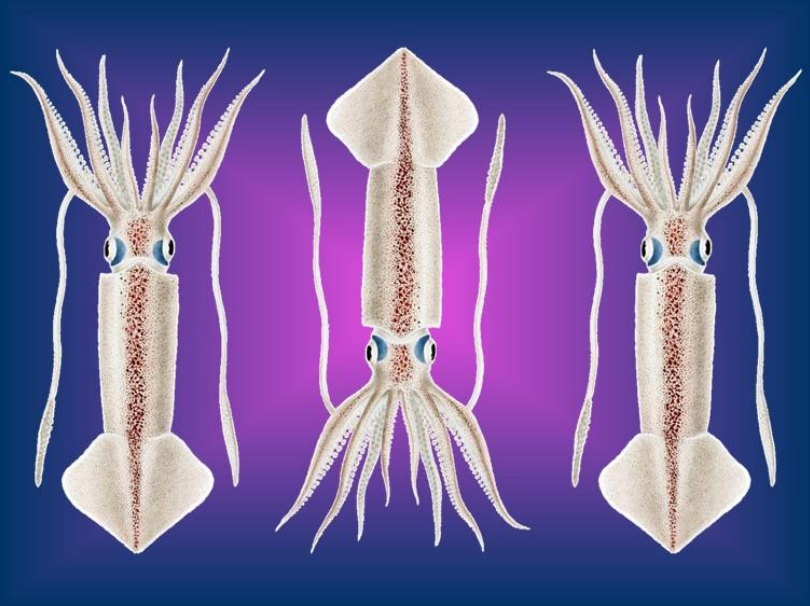

Frane Skeljo · Andreas Winter

Natural Resources - Fisheries
Falkland Islands Government
Stanley, Falkland Islands

October 2023

S2 - 2023 - LOL

Index

Summary

1) The 2023 second season *Doryteuthis gahi* fishery (X license) was open from July 30th and closed by emergency order on August 29th. Compensatory flex days for mechanical breakdown and bad weather were voided after August 29th.
2) 15,513 tonnes *D. gahi* catch was reported in the 2023 X-license fishery, giving an average CPUE of 34.3 t vessel-day^{-1}. Total catch was lowest and average CPUE second-lowest among the most recent 5 second seasons. 78.5% of *D. gahi* catch and 69.0% of fishing effort were taken south of 52º S; 21.5% of *D. gahi* catch and 31.0% of fishing effort were taken north of 52º S.
3) In the south sub-area, two depletion periods / immigration peaks were inferred on July 30th (start of the season), and August 24th. In the north sub-area, three depletion periods / immigrations were inferred on July 30th, August 13th, and August 19th.
4) Approximately 6,503 tonnes of *D. gahi* (95% confidence interval: 4,096 to 14,592 t) were estimated to have immigrated into the Loligo Box after the start of second season 2023, of which 1,330 t in the south sub-area and 5,173 t in the north sub-area.
5) The escapement biomass estimate for *D. gahi* remaining in the Loligo Box at the end of second season 2023 was: Maximum likelihood 10,996 tonnes, with a 95% confidence interval of 8,765 to 26,085 tonnes.
   The risk of *D. gahi* escapement biomass at the end of the season being less than 10,000 tonnes was estimated at 10.0%.

Introduction

Second season (X licence) of the 2023 *Doryteuthis gahi* fishery (Patagonian longfin squid – colloquially *Loligo*) opened on July 30th. Throughout the season, 36 compensatory days were requested by sixteen of the vessels, of which 15 on August 4th and 16 on August 6th (Figure 1). Compensatory days were voided after August 29th, when the season was closed by emergency order because of low biomass.

All X-licensed vessels were required to embark a Marine Mammal Observer to monitor presence and incidental capture of pinnipeds, and as now standard protocol, seal exclusion devices (SEDs) were mandatory for the duration of the season. Ultimately, 3 pinniped mortalities and 34 live releases were reported for the season: 2 (20) South American fur seals *Arctocephalus australis*, and 1 (14) Southern sea lions *Otaria flavescens*.

Total reported *D. gahi* catch under second season X licence was 12,172.7 south + 3,340.4 north = 15,513.1 tonnes, corresponding to an average CPUE of 15,513 / 452 = 34.3 tonnes vessel-day^{-1}. Total catch was lowest and average CPUE second-lowest among the most recent 5 second seasons (2019 to 2023) (Table 1).

Assessment of the Falkland Islands *D. gahi* stock was conducted with depletion time-series models as in previous seasons (Agnew et al. 1998, Roa-Ureta and Arkhipkin 2007, Arkhipkin et al. 2008), and in other squid fisheries (cited in Arkhipkin et al. 2021). Because *D. gahi* has an annual life cycle (Patterson 1988, Arkhipkin 1993), stock cannot be derived from a standing biomass carried over from prior years (Rosenberg et al. 1990, Pierce and Guerra 1994). The depletion model instead calculates an estimate of population abundance over time by evaluating what levels of abundance and catchability must be present to sustain the observed rate of catch. Depletion modelling of the *D. gahi* target fishery is used in-season, for projection, and for post-season analysis, with the objective of maintaining an escapement biomass of 10,000 tonnes *D. gahi* at the end of each season as a conservation threshold (Agnew et al. 2002, Barton 2002).

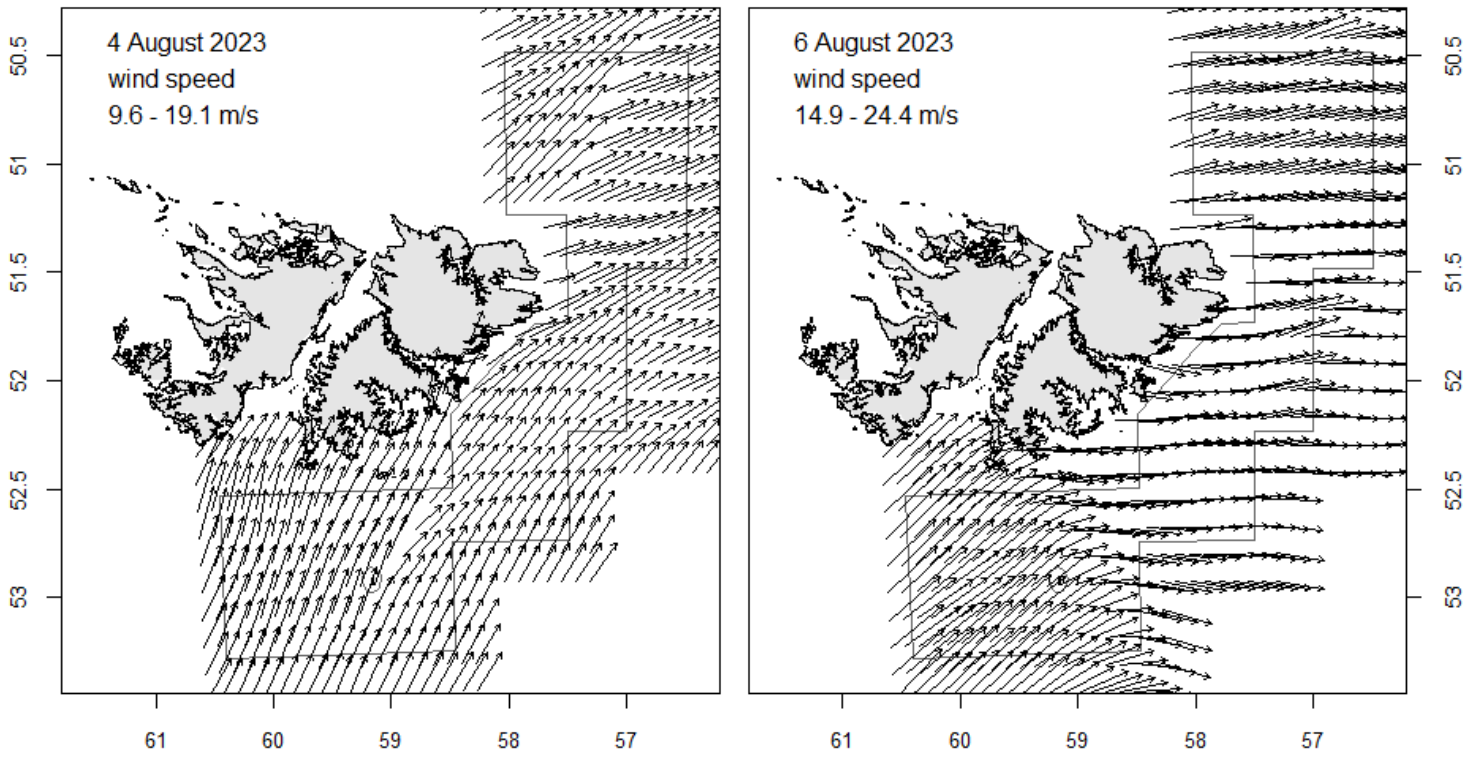

Figure 1. Wind speed vector plots (Copernicus Marine Service) on August 4th (left), when only one vessel fished, and August 6th (right), when no vessels fished.

Table 1. *D. gahi* season comparisons since 2004, when catch management was assumed by the FIFD. Days: total number of calendar days open to licensed *D. gahi* fishing including (since 1st season 2013) optional flex days; V-Days: aggregate number of licensed *D. gahi* fishing days reported by all vessels for the season. Entries in italics are seasons closed by emergency order.

	Season 1			Season 2		
	Catch (t)	Days	V-Days	Catch (t)	Days	V-Days
2004	7,152	46	625	17,559	78	1271
2005	24,605	45	576	29,659	78	1210
2006	19,056	50	704	*23,238*	*53*	*883*
2007	17,229	50	680	*24,171*	*63*	*1063*
2008	24,752	51	780	26,996	78	1189
2009	12,764	50	773	*17,836*	*59*	*923*
2010	28,754	50	765	36,993	78	1169
2011	15,271	50	771	*18,725*	*70*	*1099*
2012	34,767	51	770	35,026	78	1095
2013	19,908	53	782	19,614	78	1195
2014	28,119	59	872	19,630	71	1099
2015	*19,383*	*57*	*871*[A]	*10,190*	*42*	*665*
2016	22,616	68	1020	23,089	68	1004
2017	39,433	68	999[B]	24,101	69	1002[C]
2018	43,085	69	975	35,828	68	977
2019	55,586	68	953	*24,748*	*43*	*635*
2020	29,116	68	1012	29,759	69	993
2021	*59,587*	*62*	*891*	34,750	68	982[D]
2022	56,417	68	966[E]	43,216	68	982
2023	52,704	67	972	*15,513*	*31*	*452*

[A] Does not include C-license catch or effort after the target was switched from *D. gahi* to *Illex*.
[B] Includes two vessel-days of experimental fishing for juvenile toothfish.
[C] Includes one vessel-day of experimental fishing for juvenile toothfish.
[D] Includes three vessel-days of experimental fishing for SED improvement.
[E] Includes three vessel-days of exploratory fishing north of the Loligo Box.

Methods

The depletion model formulated for the Falklands *D. gahi* stock is based on the equivalence:

$$C_{day} = q \times E_{day} \times N_{day} \times e^{-M/2} \quad \textbf{(1)}$$

where q is the catchability coefficient, M is the natural mortality rate (considered constant at 0.0133 day^{-1}; Roa-Ureta and Arkhipkin 2007), and C_{day}, E_{day}, N_{day} are respectively catch (numbers of squid), fishing effort (numbers of vessels), and abundance (numbers of squid) per day. The catchability coefficient q summarized the range of variation of all trawls taken by the fishing fleet in this season.

In its basic form (DeLury 1947) the depletion model assumes a closed population in a fixed area for the duration of the assessment. However, the assumption of a closed population is imperfectly met in the Falkland Islands fishery, where stock analyses have often shown that *D. gahi* groups arrive in successive waves after the start of the season (Arkhipkin et al. 2021). Arrivals of successive groups are inferred from discontinuities in the catch data. Fishing on a single, closed cohort would be expected to yield gradually decreasing CPUE, but gradually increasing average individual sizes, as the squid grow. When instead these data change suddenly, or in contrast to expectation, the immigration of a new group to the population is indicated (Winter and Arkhipkin 2015).

In the event of a new group arrival, the depletion calculation must be modified to account for this influx. Modification is done using a simultaneous algorithm that adds new arrivals on top of the stock previously present, and posits a common catchability coefficient for the entire depletion time-series. If two depletions are included in the same model (i.e., the stock present from the start plus a new group arrival), then:

$$C_{day} = q \times E_{day} \times (N1_{day} + (N2_{day} \times i2|_0^1)) \times e^{-M/2} \quad \textbf{(2)}$$

where i2 is a dummy variable taking the values 0 or 1 if 'day' is before or after the start day of the second depletion. For more than two depletions, $N3_{day}$, i3, $N4_{day}$, i4, etc., would be included following the same pattern.

The season depletion likelihood function was calculated as the difference between actual catch numbers reported and catch numbers predicted from the model (Equation **2**), statistically corrected by a factor relating to the number of days of the depletion period (Roa-Ureta 2012):

$$\text{minimization} \rightarrow \ ((n\text{Days} - 2)/2) \times \log\left(\sum_{days}\left(\log(\text{predicted } C_{day}) - \log(\text{actual } C_{day})\right)^2\right) \quad \textbf{(3)}$$

The stock assessment was set in a Bayesian framework (Punt and Hilborn 1997), whereby results of the season depletion model are conditioned by prior information on the stock; in this case the information from the pre-season survey.

The likelihood function of prior information was calculated as the normal distribution of the difference between catchability derived from the survey abundance estimate ($_{prior}\,q$), and catchability derived from the season depletion model ($_{depletion}\,q$). Applying this difference requires both the survey and the season to be fishing the same stock with the same gear. Catchability, rather than abundance N, is used for calculating prior likelihood because catchability informs the entire season time series; whereas N from the survey only informs the first in-season depletion period – subsequent immigrations and depletions are independent of the abundance that was present during the survey. Thus, the prior likelihood function was:

$$\text{minimization} \rightarrow \frac{1}{\sqrt{2\pi \cdot SD_{prior\ q}{}^2}} \times \exp\left(-\frac{\left({}_{depletion}\,q - {}_{prior}\,q\right)^2}{2 \cdot SD_{prior\ q}{}^2}\right) \quad \textbf{(4)}$$

where the standard deviation of catchability prior ($SD_{prior\ q}$) was calculated from the Euclidean sum (Carlson 2014) of the survey prior estimate uncertainty, the variability in catches on the season start date, and the uncertainty in the natural mortality M estimate over the number of days mortality discounting (Appendix Equation **A5**).

Bayesian optimization of the depletion was calculated by jointly minimizing Equations **3** and **4**, using the Nelder-Mead algorithm in R programming package 'optimx' (Nash and Varadhan 2011). Relative weights in the joint optimization were assigned to Equations **3** and **4** as the converse of their coefficients of variation (CV), i.e., the CV of the prior became the weight of the depletion model and the CV of the depletion model became the weight of the prior. Calculations of the depletion CVs are described in Equations **A8-S** and **A8-N**. Because a complex model with multiple depletions may converge on a local minimum rather than global minimum, the optimization was stabilized by running a feed-back loop that set the q and N parameter outputs of the Bayesian joint optimization back into the in-season-only minimization (Equation **3**), re-calculated the in-season-only minimization, then re-calculated the Bayesian joint optimization, and continued this process until both the in-season minimization and the joint optimization remained unchanged.

With actual C_{day}, E_{day} and M being fixed parameters, the optimization of Equation **2** using Equations **3** and **4** produces estimates of q and N1, N2, …, etc. Numbers of squid on the final day (or any other day) of a time series are then calculated as the numbers N of the depletion start days discounted for natural mortality during the intervening period, and subtracting cumulative catch also discounted for natural mortality (CNMD). Taking for example a two-depletion period:

$$\begin{aligned} N_{final\ day} &= N1_{start\ day\ 1} \times e^{-M\ (final\ day - start\ day\ 1)} \\ &+ N2_{start\ day\ 2} \times e^{-M\ (final\ day - start\ day\ 2)} \\ &- CNMD_{final\ day}, \end{aligned} \quad \textbf{(5)}$$

$$CNMD_{day\ 1} = 0$$

$$CNMD_{day\ x} = CNMD_{day\ x-1} \times e^{-M} + C_{day\ x-1} \times e^{-M/2} \quad \textbf{(6)}$$

$N_{final\ day}$ is then multiplied by the average individual weight of squid on the final day to give biomass. Daily average individual weight is obtained from length / weight conversion of mantle lengths measured in-season by observers, and also derived from in-season commercial data as the proportion of product weight that vessels reported per market size category[a]. Observer

[a] First reported for Falkland Islands *D. gahi* by Payá (2006). Also used in some finfish commercial fisheries, see Plet-Hansen et al. 2018.

mantle lengths are scientifically more accurate, but restricted to a partial sample of trawls. Commercially proportioned mantle lengths are relatively less accurate, but cover every trawl of the entire fishing fleet every day. Therefore, both sources of data are used (see Appendix – *Doryteuthis gahi* individual weights).

Distributions of the likelihood estimates from joint optimization (i.e., measures of their statistical uncertainty) were computed using a Markov Chain Monte Carlo (MCMC) (Gamerman and Lopes 2006), a method that is commonly employed for fisheries assessments (Magnusson et al. 2013). MCMC is an iterative process which generates random stepwise changes to the proposed outcome of a model (in this case, the q and N of *D. gahi* squid) and at each step, accepts or nullifies the change with a probability equivalent to how well the change fits the model parameters compared to the previous step. The resulting sequence of accepted or nullified changes (i.e., the 'chain') approximates the likelihood distribution of the model outcome. The MCMC of the depletion models were run for 200,000 iterations; the first 1000 iterations were discarded as burn-in sections (initial phases over which the algorithm stabilizes); and the chains were thinned by a factor equivalent to the maximum of either 5 or the inverse of the acceptance rate (e.g., if the acceptance rate was 12.5%, then every eighth (0.125^{-1}) iteration was retained) to reduce serial correlation. For each model three chains were run; one chain initiated with the parameter values obtained from the joint optimization of Equations **3** and **4**, one chain initiated with these parameters ×2, and one chain initiated with these parameters ×¼. Convergence of the three chains was accepted if the variance among chains was less than 10% higher than the variance within chains (Brooks and Gelman 1998). When convergence was satisfied the three chains were combined as one final set. Equations **5**, **6**, and the multiplication by average individual weight were applied to the CNMD and to each iteration of N values in the final set, and the biomass outcomes from these calculations represent the distribution of the estimate.

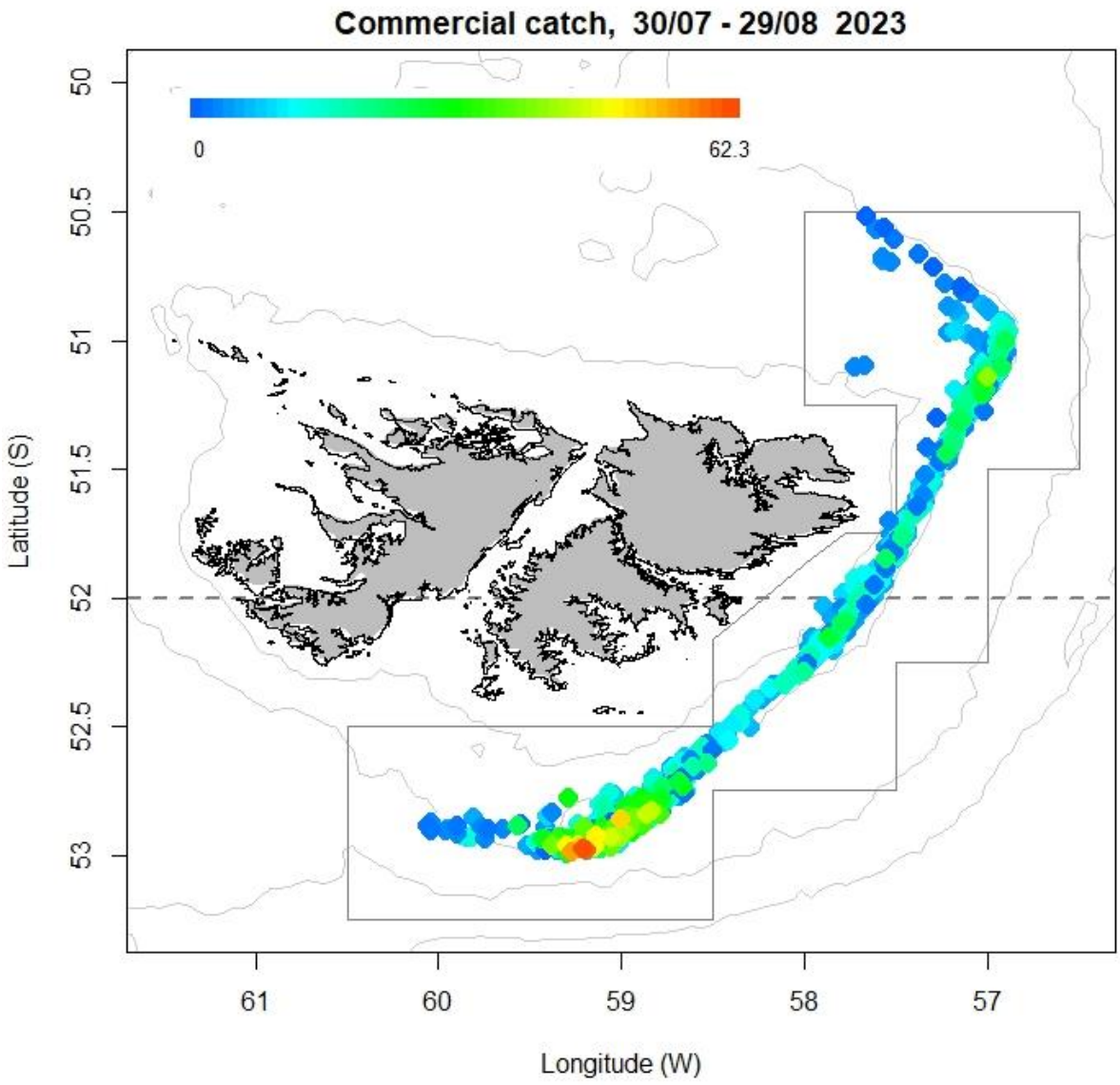

Figure 2. Spatial distribution of *D. gahi* second-season trawls (mean coordinate positions), colour-scaled to catch weight (max. = 62.3 tonnes). 1246 trawl catches were taken during the season. The Loligo Box fishing zone and 52 ºS parallel delineating the boundary between north and south assessment sub-areas, are shown in grey.

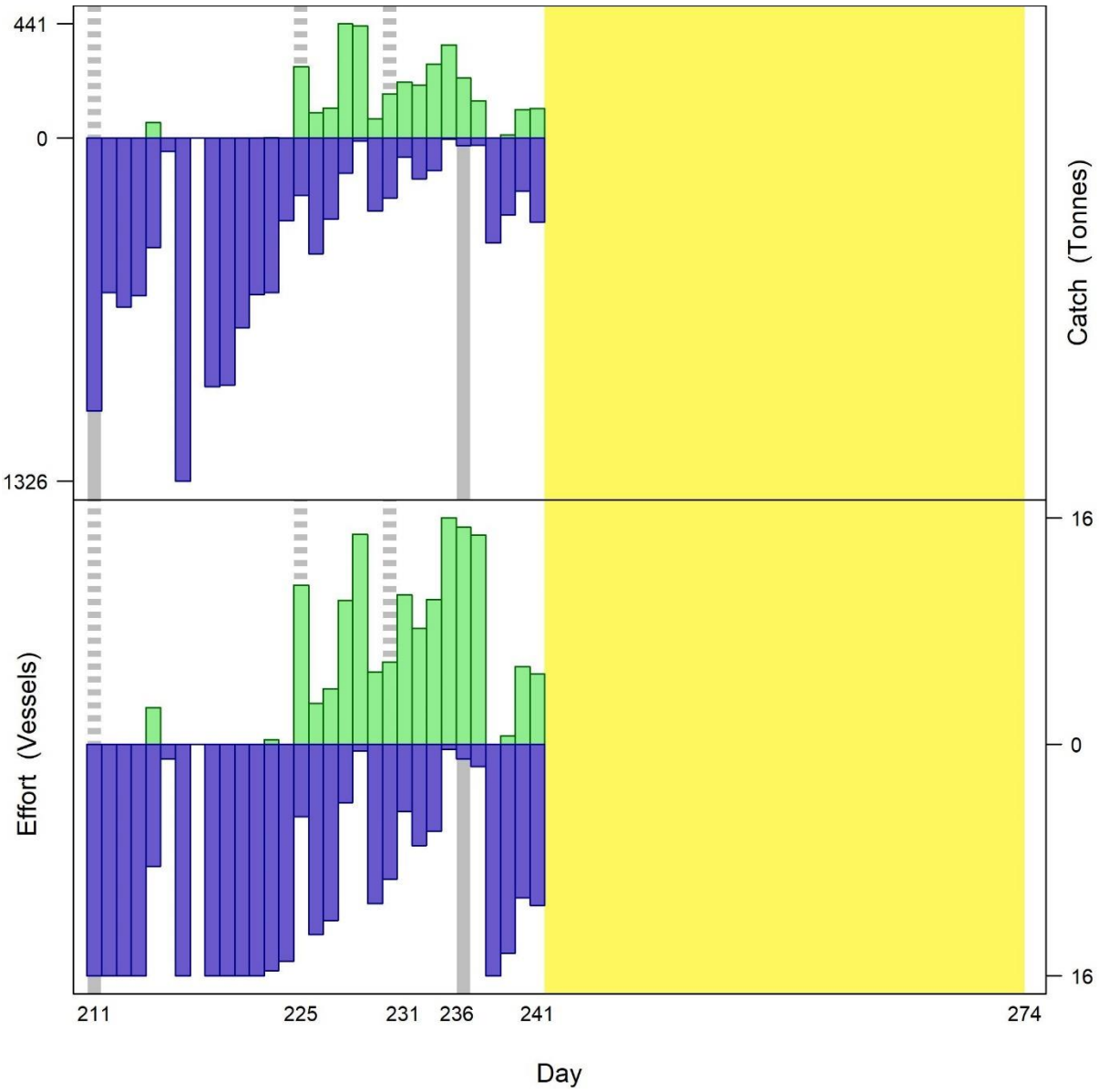

Figure 3. Daily total *D. gahi* catch and effort distribution by assessment sub-area north (green) and south (purple) of the 52º S parallel during second season 2023. The season was open from July 30th (chronological day 211) with directed closure on October 1st (day 274), but closed by emergency order after August 29th (day 241). As many as 16 vessels fished per day north; as many as 16 vessels fished per day south. Yellow under-shading: early closures of the north and south sub-areas. As much as 441 tonnes *D. gahi* was caught per day north; as much as 1326 tonnes *D. gahi* was caught per day south.

Depletion models and likelihood distributions were calculated separately for north and south sub-areas of the Loligo Box fishing zone, as *D. gahi* sub-stocks emigrate from different spawning grounds and remain to an extent segregated (Arkhipkin and Middleton 2002), although they represent a single intermixed population (Shaw et al. 2004). However, q_{prior} was calculated for the north and south sub-areas combined, rather than separately (Equation **A4**). As fishing tends to start predominantly in one or the other sub-area, rather than the fleet spreading itself evenly, separately computed north and south qs_{prior} are susceptible to arbitrary differences. Total escapement biomass was then defined as the aggregate biomass of *D. gahi* on the last day of the season for north and south sub-areas combined, with north and south likelihood distributions added together randomly.

Stock assessment

Catch and effort

The north sub-area was fished on 18 of 31 season-days, for 21.5% of total catch (3340.4 tonnes *D. gahi*) and 31.0% of effort (140.0 vessel-days); both percentages below median since 2010 (Figures 2 and 3). Only about one-tenth of north sub-area catch or effort were taken during the first half of the season. The south sub-area was fished on 30 of the 31 season-days, for 78.5% of total catch (12172.7 t *D. gahi*) and 69.0% of effort (312.0 vessel-days).

Data

452 vessel-days were fished during the season (Table 1), with a median of 16 vessels per day (mean 14.6). Vessels reported daily catch totals to the FIFD and electronic logbook data that included trawl times, positions, depths, and product weight by market size categories. Two FIG fishery observers were deployed on two vessels in the fishing season for a total of 21 sampling days[b] (Nicholls 2023, Amukwaya 2023). Throughout the 31 days of the season, 10 days had no FIG fishery observer sampling, and 21 days had 1 FIG fishery observer sampling. Except for seabird days FIG fishery observers were tasked with sampling 200 *D. gahi* at two stations daily; reporting their maturity stages, sex, and lengths to 0.5 cm. Contract marine mammal observers were tasked with measuring 100 unsexed lengths of *D. gahi* per day. The length-weight relationship for converting observer and commercially proportioned lengths was combined from second pre-season and season length-weight data of both 2022 and 2023, as 2023 data became available progressively with on-going observer coverage. The final parameterization of the length-weight relationship included 4896 measures from 2022 and 3118 measures from 2023, giving:

$$\text{weight (kg)} = 0.16372 \times \text{length (cm)}^{2.21687} / 1000 \quad \textbf{(7)}$$

with a coefficient of determination $R^2 = 90.4\%$.

Group arrivals / depletion criteria

Start days of depletions - following arrivals of new *D. gahi* groups - were judged primarily by daily changes in CPUE, with additional information from sex proportions, maturity, and average individual squid sizes. CPUE was calculated as metric tonnes of *D. gahi* caught per vessel per day. Days were used rather than trawl hours as the basic unit of effort. Commercial vessels do not trawl standardized duration hours, but rather durations that best suit their daily processing requirements. An effort index of days is therefore more consistent (FIFD 2004, Winter and Arkhipkin 2015). Inclusion of additional depletion starts was partially evaluated by improvement of the Akaike information criterion (AIC; Akaike 1973) on model fit.

Two days south and three days north were identified that represented the onset of significant immigrations / depletions throughout the season. The day of highest CPUE all season (day 217, August 5th) was determined to represent a biomass concentration, and not an immigration, between two days of severe weather (Figure 1). Catches and CPUE increased again on the last day in the south, but average individual squid sizes did not corroborate that this increase represented an immigration.

[b] Not counting seabird days (every fourth day).

- The first depletion start south was set by definition on day 211 (July 30th), the first day of the season with all sixteen vessels fishing south. CPUE was the second-highest all season (Figure 4), and average maturities were lowest of the season (Figure 5D).
- The second depletion start south was identified on day 236 (August 24th), as CPUE increased sharply after a period of decline (Figure 4), and average individual squid weights decreased to the near-lowest all season (Figure 5A, B).
- The first depletion start north was set by definition on day 211 (July 30th), although no fishing in the north occurred until four days later (Figure 4).
- The second depletion start north was identified on day 225 (August 13th), the first time since onset of the season that more than three vessels fished in the north. CPUE and average individual squid weights were average (Figures 4, 5A, 5B).
- The third depletion start north was identified on day 231 (August 19th), with a small peak in CPUE (Figure 4), local minima in average individual squid weights (Figure 5A, B), near the maximum of female proportion (Figure 5C), and a dip in average female maturity (Figure 5D).

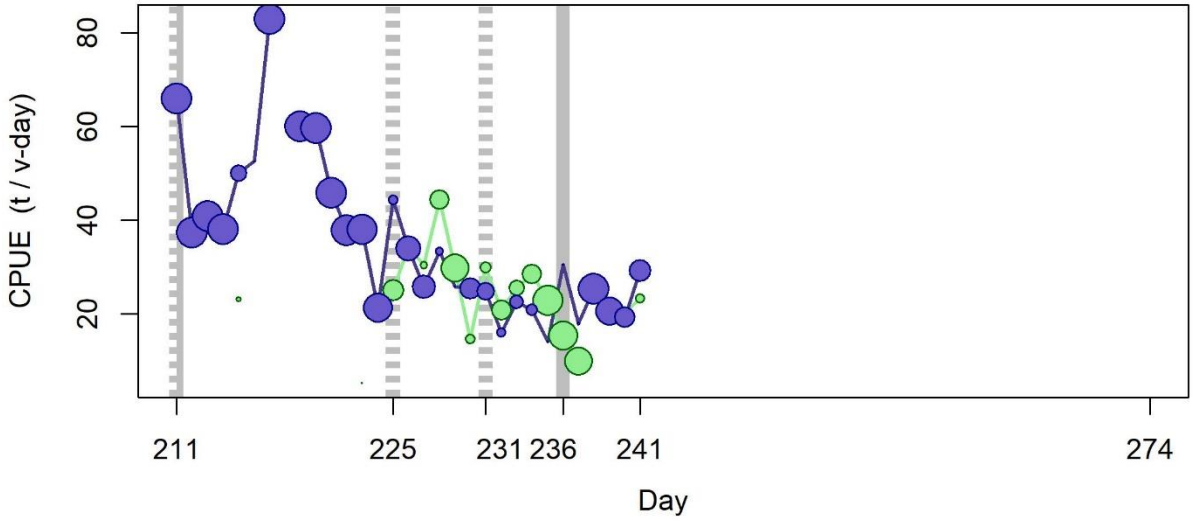

Figure 4. CPUE in metric tonnes per vessel per day, by assessment sub-area north (green) and south (purple) of 52º S latitude. Circle sizes are proportioned to numbers of vessels fishing. Data from consecutive days are joined by line segments. Broken grey bars indicate the starts of in-season depletions north. Solid grey bars indicate the starts of in-season depletions south.

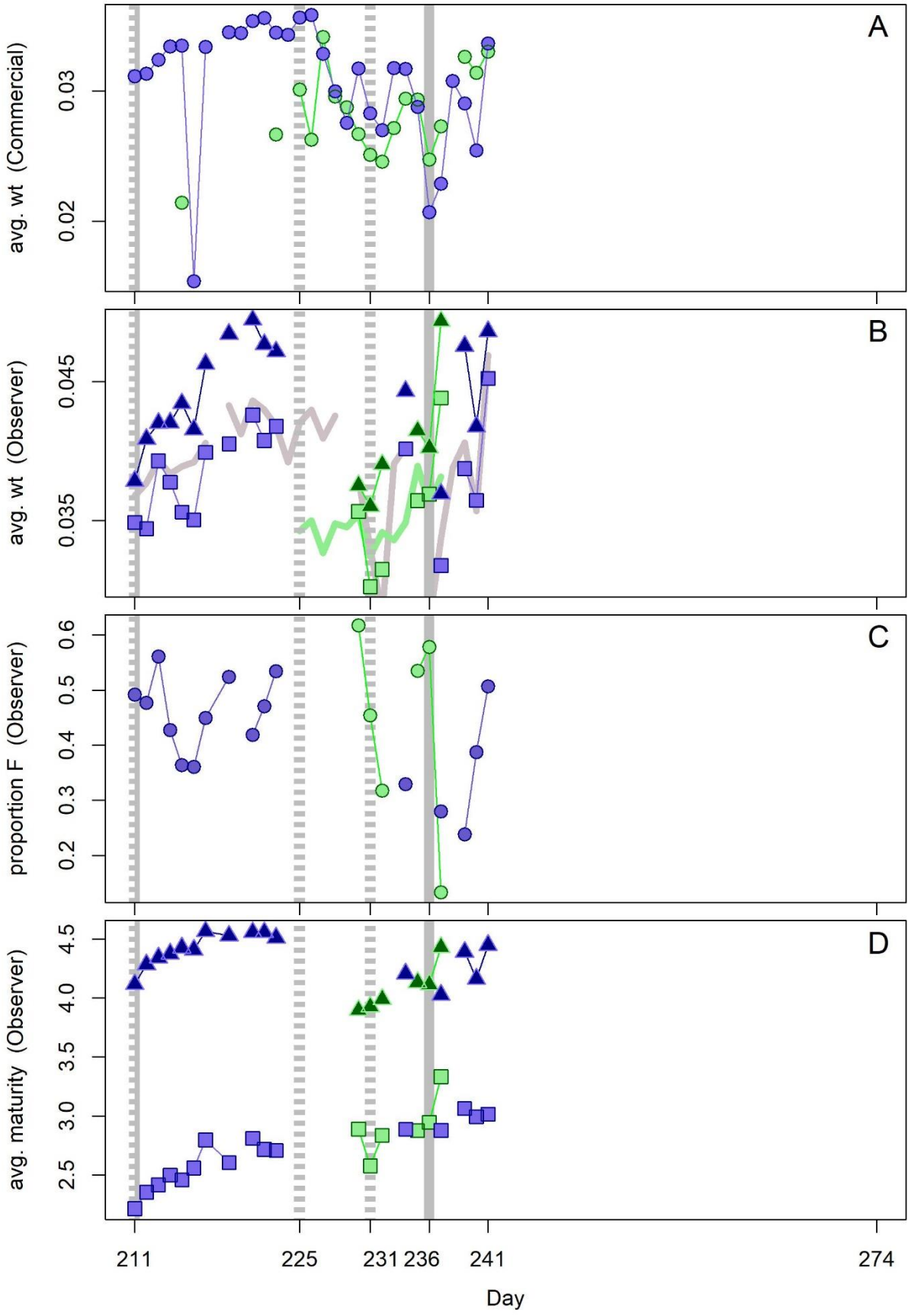
A
B
C
D
avg. wt (Commercial)
avg. wt (Observer)
proportion F (Observer)
avg. maturity (Observer)
0.02
0.03
0.035
0.045
0.2
0.3
0.4
0.5
0.6
2.5
3.0
3.5
4.0
4.5
211
225
231
236
241
274
Day

Figure 5 [previous page]. A: Average individual *D. gahi* weights (kg) per day from commercial size categories. B: Average individual *D. gahi* weights (kg) by sex per day from FIG observer sampling. C: Proportions of female *D. gahi* per day from observer sampling. D: Average maturity index value (Lipiński 1979) by sex per day from observer sampling. Males: triangles, females: squares, combined: circles. Thick lines (B) are unsexed measurements from the contract marine mammal observers. North sub-area: green, south sub-area: purple. Data from consecutive days are joined by line segments. Broken grey bars: starts of in-season depletions north. Solid grey bars: starts of in-season depletions south.

Depletion analyses
South

In the south sub-area, the maximum likelihood posterior ($_{Bayesian}\ q_S = 3.137 \times 10^{-3}$; Figure 6-left, and Equation **A9-S**) was preponderantly optimized on the in-season depletion ($_{depletion}\ q_S = 3.119 \times 10^{-3}$; Figure 6-left, and Equation **A6-S**), which had about 3× higher weight than the prior ($_{prior}\ q = 3.238 \times 10^{-3}$; Figure 6-left, and Equation **A4**) in the Bayesian model (Equations **A5** and **A8-S**).

The MCMC distribution of the Bayesian posterior multiplied by the generalized additive model (GAM) fit of average individual squid weight (Figure A1-south) gave the likelihood distribution of *D. gahi* biomass on day 241 (August 29th) shown in Figure 6-right, with maximum likelihood and 95% confidence interval of:

$$B_{S\ day\ 241} = 6{,}713\ t \sim 95\%\ CI\ [4{,}697 – 13{,}349]\ t \quad \textbf{(8-S)}$$

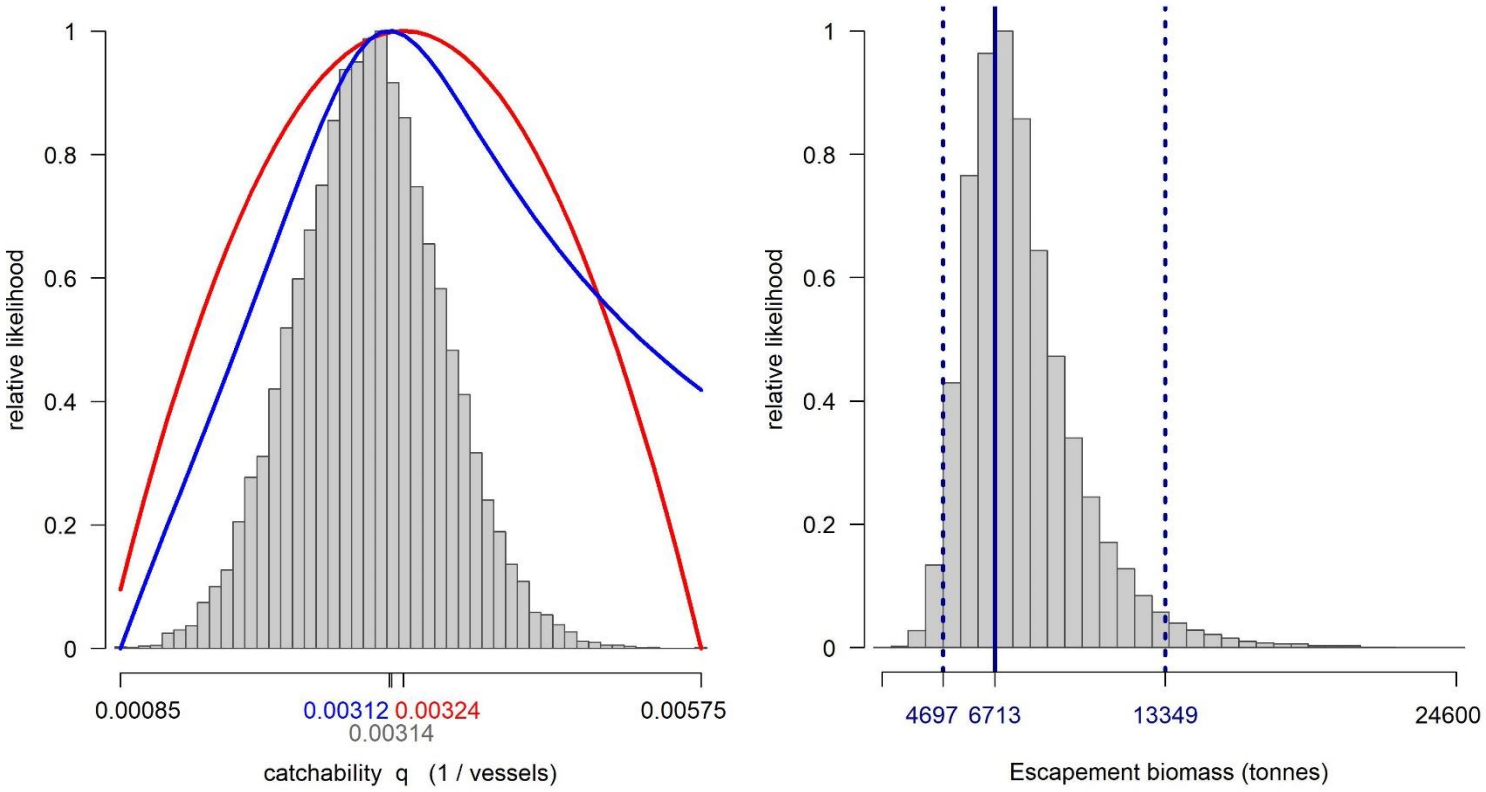

Figure 6 [previous page]. South sub-area. Left: Likelihood distributions for *D. gahi* catchability. Red line: prior model (pre-season survey data), blue line: in-season depletion model, grey bars: combined Bayesian model posterior. Right: Likelihood distribution (grey bars) of escapement biomass, from Bayesian posterior and average individual squid weight at the end of the season. Blue lines: maximum likelihood and 95% confidence interval. Note correspondence to Figure 7.

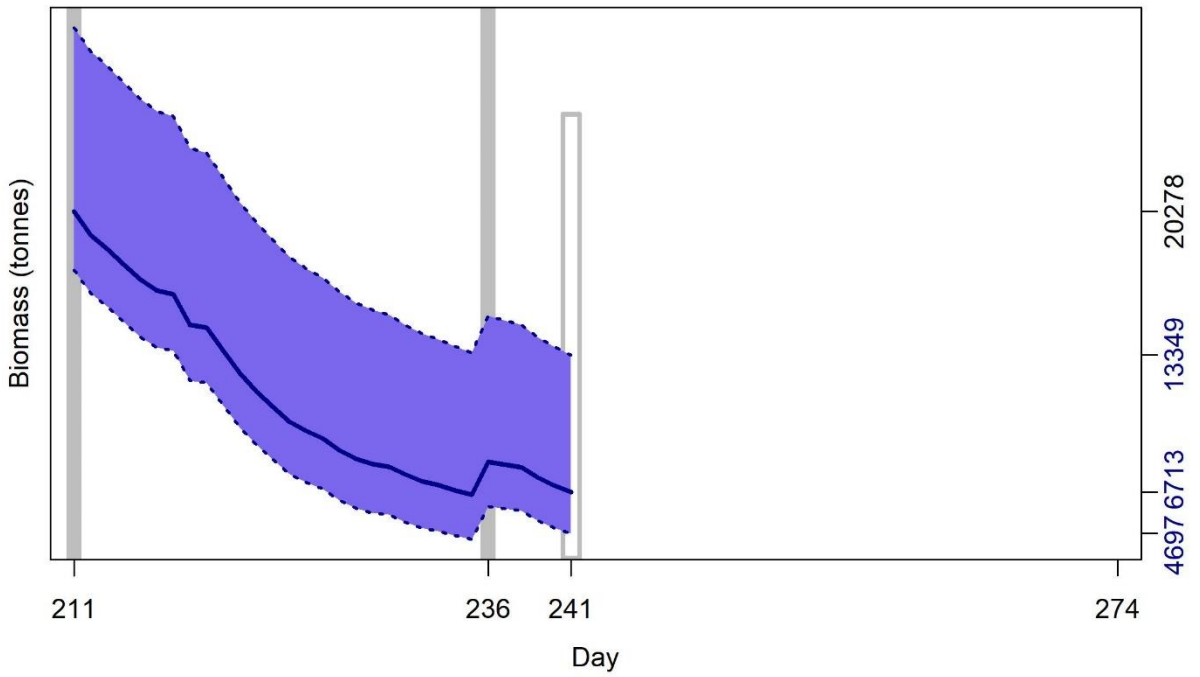

Figure 7. South sub-area. *D. gahi* biomass time series estimated from Bayesian posterior of the depletion model ± 95% confidence interval. Grey bars indicate the start of in-season depletions south; days 211 and 236. Note that the biomass 'footprint' on day 241 (August 29th) corresponds to the right-side plot of Figure 6.

On the first day of the season estimated *D. gahi* biomass south was 20,278 t ~ 95% CI [17,452 – 29,203] t (Figure 7); marginally significantly higher (p = 0.074) than the pre-season estimate of 14,913 t [10,230 – 22,040] (Chemshirova et al. 2023). The highest biomass estimate of the season occurred with the first immigration on day 211.

North

In the north sub-area, the maximum likelihood posterior ($_{\text{Bayesian}}\, q_N = 4.254 \times 10^{-3}$; Figure 8-left, and Equation **A9-N**) was preponderantly optimized on the prior ($_{\text{prior}}\, q = 3.238 \times 10^{-3}$; Figure 8-left, and Equation **A4**). Comparably to the south, the in-season depletion had about 2.5× higher weight than the prior in the Bayesian model (Equations **A5** and **A8-N**), but the in-season depletion ($_{\text{depletion}}\, q_N = 7.501 \times 10^{-3}$; Figure 8-left, and Equation **A6-N**) was weakly defined (Figure 4). A particular circumstance in the north is that from time to time vessels leave port and fish for a few hours in the afternoon to evening, catching relatively little but nevertheless counting a full fishing day according to the computational structure of the model.

The MCMC distribution multiplied by average individual weight gave the likelihood distribution of *D. gahi* biomass on day 241 (August 29th) shown in Figure 8-right, with maximum likelihood and 95% confidence interval of:

$B_{N\ day\ 241}$ = 4,356 t ~ 95% CI [2,788 – 17,747] t **(8-N)**

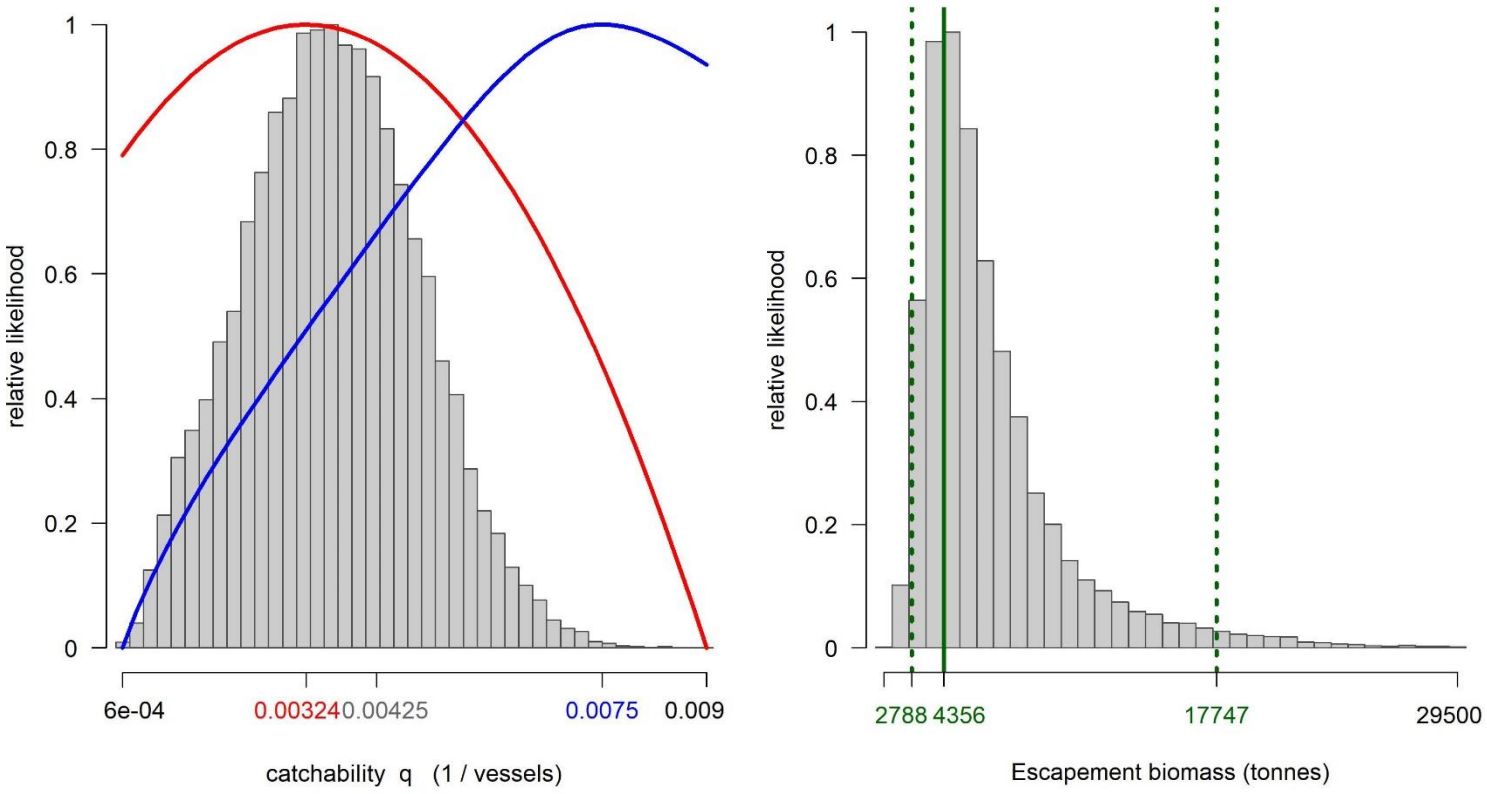

Figure 8. North sub-area. Left: Likelihood distributions for *D. gahi* catchability. Red line: prior model (pre-season survey data), blue line: in-season depletion model, grey bars: combined Bayesian model posterior. Right: Likelihood distribution (grey bars) of escapement biomass, from Bayesian posterior and average individual squid weight at the end of the season. Green lines: maximum likelihood and 95% confidence interval. Note the correspondence to Figure 9.

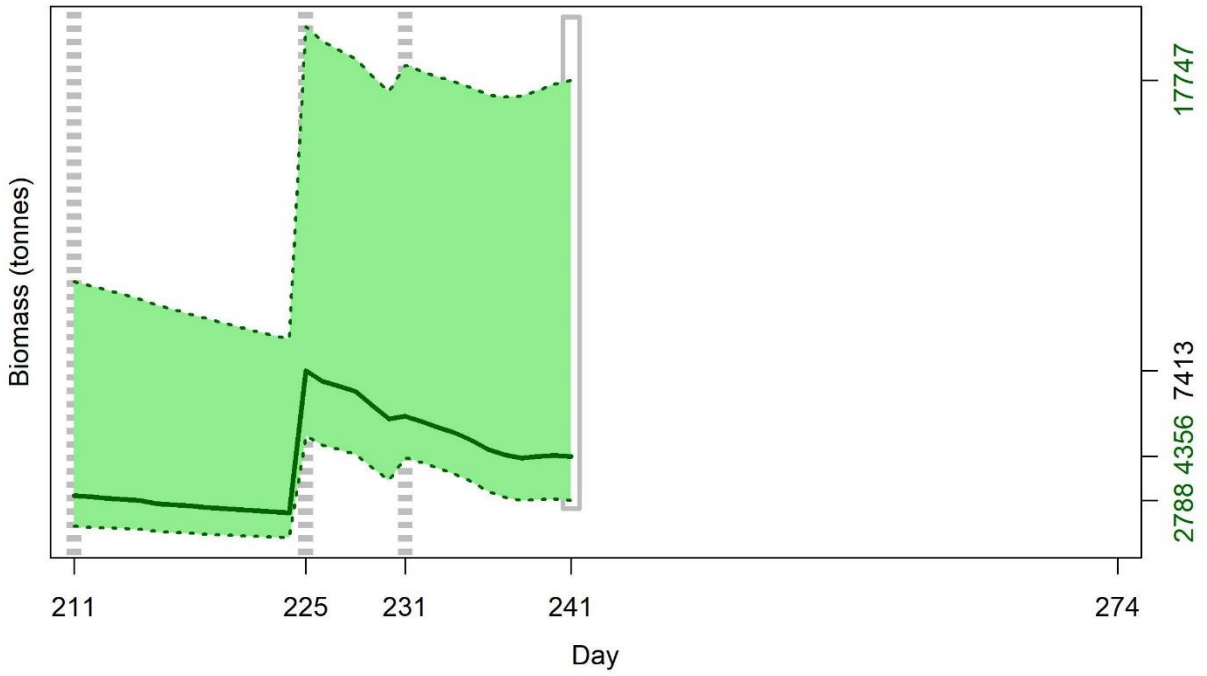

Figure 9. North sub-area. *D. gahi* biomass time series estimated from Bayesian posterior of the depletion model ± 95% confidence interval. Broken grey bars indicate the start of in-season depletions north; days 211, 225, and 231. Note that the biomass 'footprint' on day 241 (August 29th) corresponds to the right-side plot of Figure 8.

On the first day of the season estimated *D. gahi* biomass north was 2,962 t ~ 95% CI [1,874 – 10,582] t; lower but not statistically different ($p > 0.20$) than the pre-season estimate of 4,956 t [3,647 – 7,230] (Chemshirova et al. 2023). The highest biomass estimate of the season occurred with the second immigration on day 225, reaching 7,413 t [5,103 – 19,673]. Effectively, the variation of biomass estimate throughout the season was not statistically significant; by the rule that a straight line could be drawn through the plot (Figure 9) without intersecting the 95% confidence interval (Swartzman et al. 1992).

Immigration

Doryteuthis gahi immigration during the season was inferred on each day by how many more squid were estimated present than the day before, minus the number caught and the number expected to have died naturally:

$$\text{Immigration}\, N_{\text{day i}} = N_{\text{day i}} - (N_{\text{day i-1}} - C_{\text{day i-1}} - M_{\text{day i-1}})$$

where $N_{\text{day i-1}}$ are optimized in the depletion models, $C_{\text{day i-1}}$ calculated as in Equations **2** and **3**, and $M_{\text{day i-1}}$ is:

$$M_{\text{day i-1}} = (N_{\text{day i-1}} - C_{\text{day i-1}}) \times (1 - e^{-M})$$

Immigration biomass per day was then calculated as the immigration number per day multiplied by predicted average individual weight from the GAM:

$$_{\text{Immigration}}B_{\text{day i}} = {}_{\text{Immigration}}N_{\text{day i}} \times {}_{\text{GAM}}Wt_{\text{day i}}$$

All numbers N are themselves derived from the daily average individual weights, therefore the estimation automatically factors in that those squid immigrating on a given day would likely be smaller than average (because younger). Confidence intervals of the immigration estimates were calculated by applying the above algorithms to the MCMC iterations of the depletion models. Resulting total biomasses of *D. gahi* immigration north and south, up to season end (day 241), were:

$$_{\text{Immigration}}B_{\text{S season}} = 1{,}330 \text{ t} \sim 95\% \text{ CI } [-699 \text{ to } 3{,}573] \text{ t} \quad \textbf{(9-S)}$$

$$_{\text{Immigration}}B_{\text{N season}} = 5{,}173 \text{ t} \sim 95\% \text{ CI } [3{,}642 \text{ to } 13{,}008] \text{ t} \quad \textbf{(9-N)}$$

Total immigration with randomized addition of the confidence intervals was:

$$_{\text{Immigration}}B_{\text{Total season}} = 6{,}503 \text{ t} \sim 95\% \text{ CI } [4{,}096 \text{ to } 14{,}592] \text{ t} \quad \textbf{(9-T)}$$

In the south sub-area, the in-season peak on day 236 accounted for approximately 58.9% of in-season immigration (start day 211 was de facto not an in-season immigration). In the north sub-area, the in-season peaks on days 225 and 231 accounted for approximately 90.8% and 4.2% of in-season immigration. Both south and north, the remaining immigration percentages were accounted for by the minor fluctuations throughout the season.

Escapement biomass

Total escapement biomass was defined as the aggregate biomass of *D. gahi* at the end of day 241 (August 29th) for south and north sub-areas combined (Equations **8**). Depletion models are calculated on the inference that all fishing and natural mortality are gathered at mid-day, thus a half day of mortality ($e^{-M/2}$) was added to correspond to the closure of the fishery at 23:59 (mid-night) on August 29th (Equation **10)**.

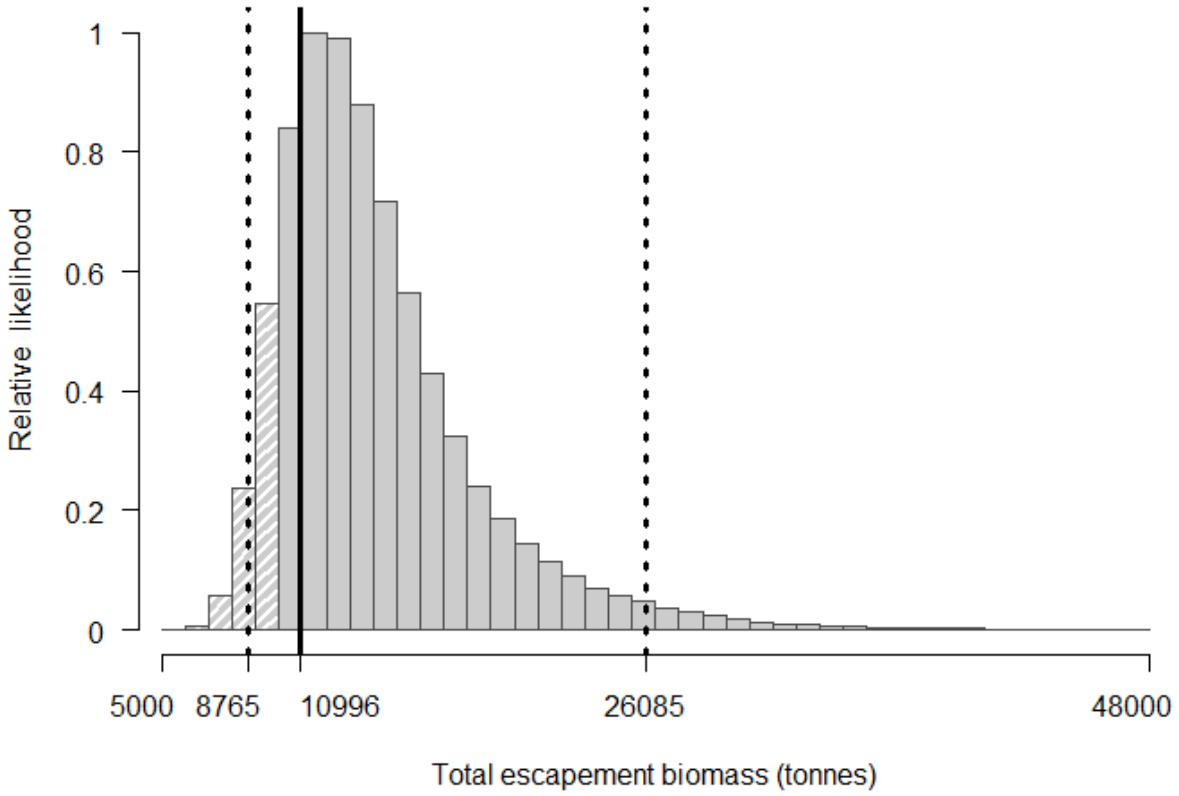

Figure 10. Likelihood distribution with 95% confidence interval of total *D. gahi* escapement biomass at the season end (August 29th). White shading lines: portion of the distribution <10,000 tonnes; equal to 10.0% of the whole distribution.

$$B_{\text{Total day 241}} = (B_{\text{S day 241}} + B_{\text{N day 241}}) \times e^{-M/2}$$

$$= 11{,}069 \text{ t} \times 0.99336$$

$$= 10{,}996 \text{ t} \sim 95\% \text{ CI } [8{,}765 – 26{,}085] \text{ t} \quad \textbf{(10)}$$

Randomized addition of the south and north distributions gave the aggregate likelihood of total escapement biomass ($B_{\text{Total day 241}}$) shown in Figure 10. With both the south and the north escapement biomass distributions being right-skewed (Figures 6-right and 8-right), the addition of the two produced an asymmetric confidence interval relative to the empirical total. The risk of the fishery in the current season, defined as the proportion of the total escapement biomass distribution below the conservation limit of 10,000 tonnes (Agnew et al. 2002, Barton 2002), was calculated as 10.0%. The estimated escapement biomass of 10,996 t was the lowest for second seasons since 2019, also closed early (Winter 2019).

The final decision to close the season was made on August 28th, based on catch and effort data through August 27th. On that date, the aggregate of north and south depletion modelling projected that estimated biomass would fall below 10,000 tonnes on August 28th (day 240; Figure 11). The typical season outcome of CPUE increasing again slightly on the last day was observed (Figure 4).

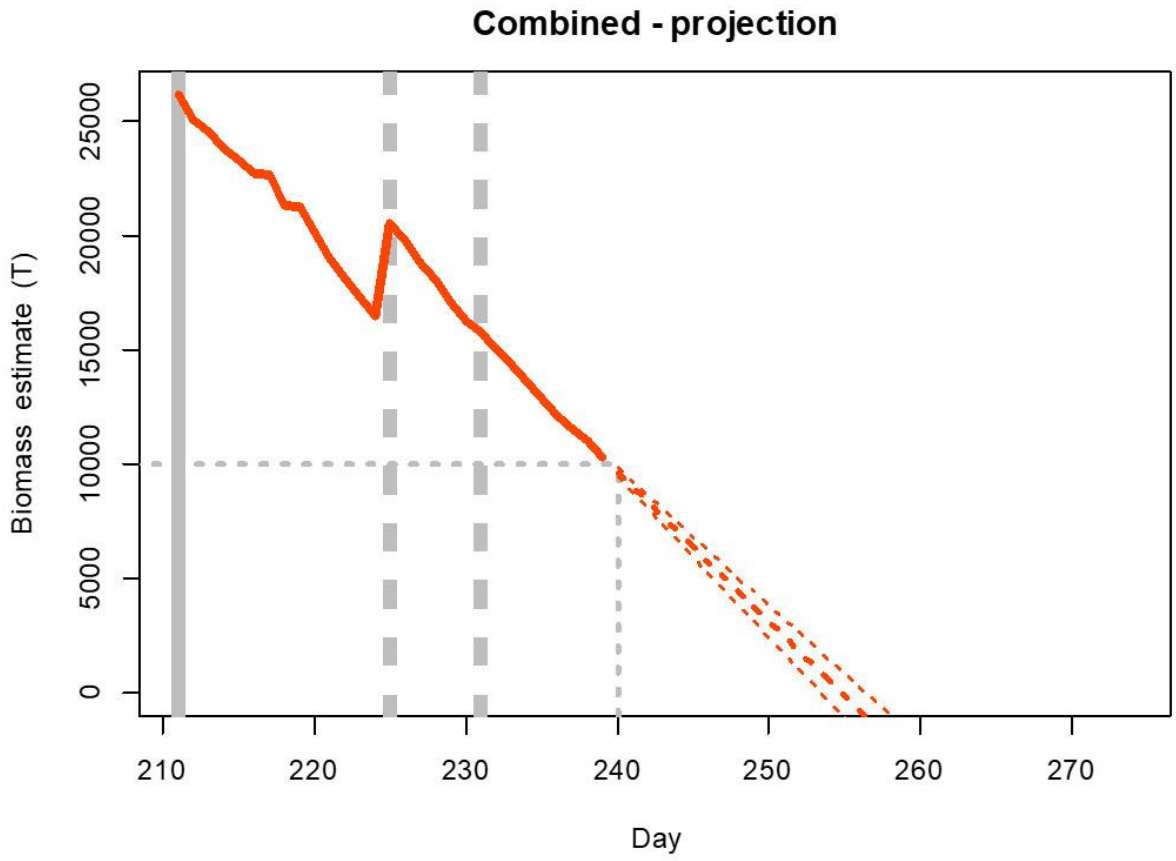

Figure 11. Depletion-modelled (solid orange line) and GAM-projected (broken orange line + 95% conf. intervals) aggregate *D. gahi* biomass calculated from data through day 239 (August 27th), showing decrease below 10000 tonnes on day 240 (August 28th). Broken and solid grey bars indicate the starts of in-season depletions. Note that the second depletion start south on day 236 (cf. Figure 3) was not confirmed yet when this projection was calculated.

Fishery bycatch

All 452 second-season vessel-days (Table 1) reported *D. gahi* squid as their primary catch. The proportion of season total catch represented by *D. gahi* (15513101/15774150 = 0.983; Table A1) was median among second seasons of the past five years, but consistent with a generally increasing trend over the past 12 years. Scallops (*Zygochlamys*) have been taking a progressively higher ranking in second-season aggregate catches since 2019; last year 2022 scallops were the third-highest second-season catch (Winter and Skeljo 2022) and this year the second-highest second-season catch (Table A1).

Figure 12 [below]. Distributions of the eight main bycatches during second season 2023, by noon position grids. Thickness of grid lines is proportional to the number of vessel-days (1 to 124 per grid; 18 different grids were occupied). Grey-scale is proportional to the season bycatch biomass per grid; maximum (tonnes) indicated on each plot.

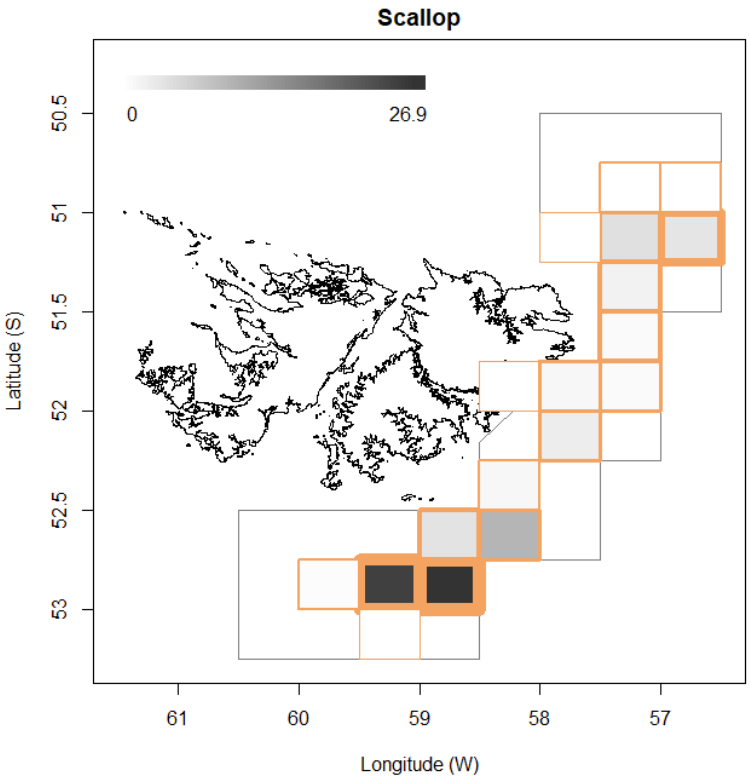
Scallop
0
26.9
Latitude (S)
50.5
51
51.5
52
52.5
53
61
60
59
58
57
Longitude (W)

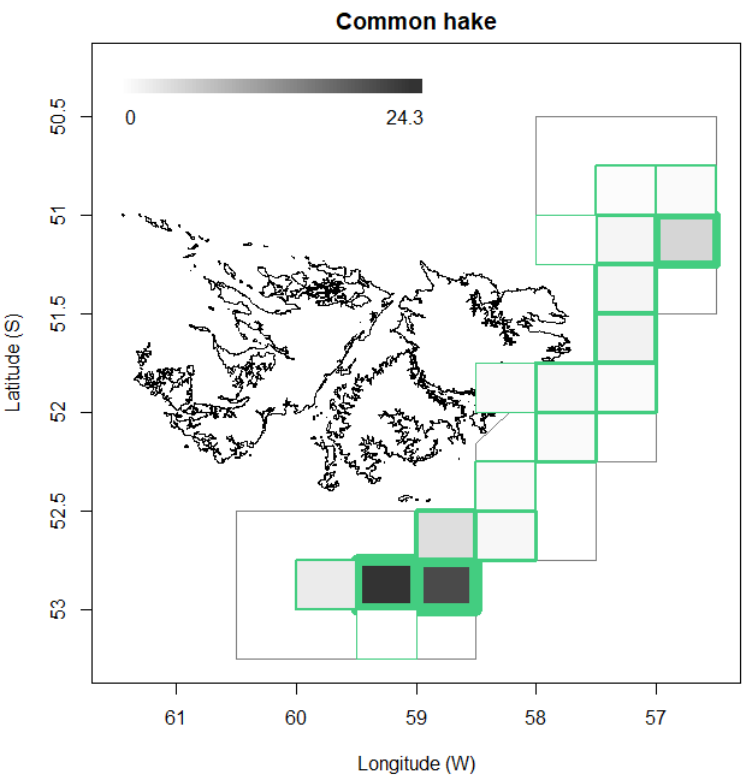
Common hake
0
24.3
Latitude (S)
50.5
51
51.5
52
52.5
53
61
60
59
58
57
Longitude (W)

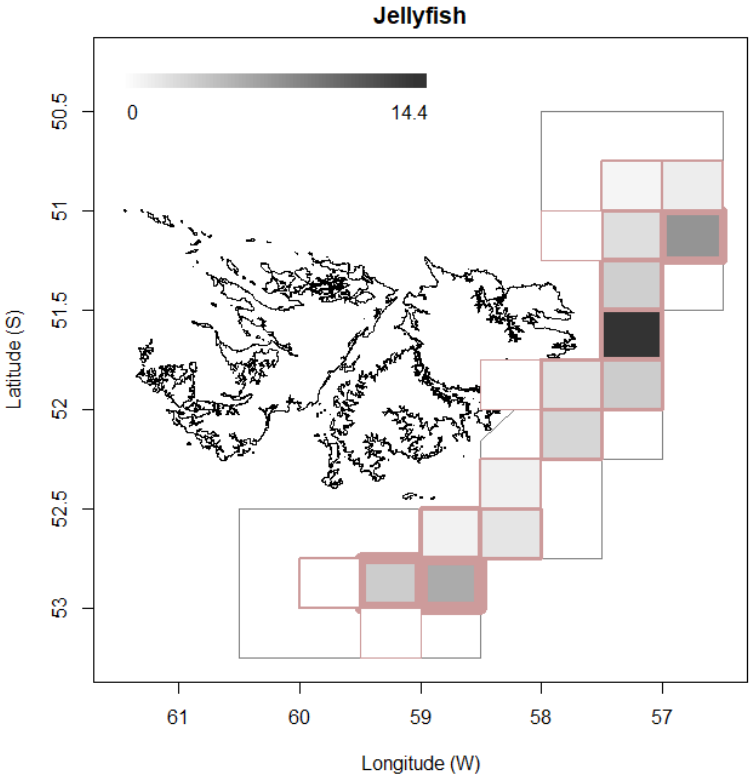
Jellyfish
0
14.4
Latitude (S)
50.5
51
51.5
52
52.5
53
61
60
59
58
57
Longitude (W)

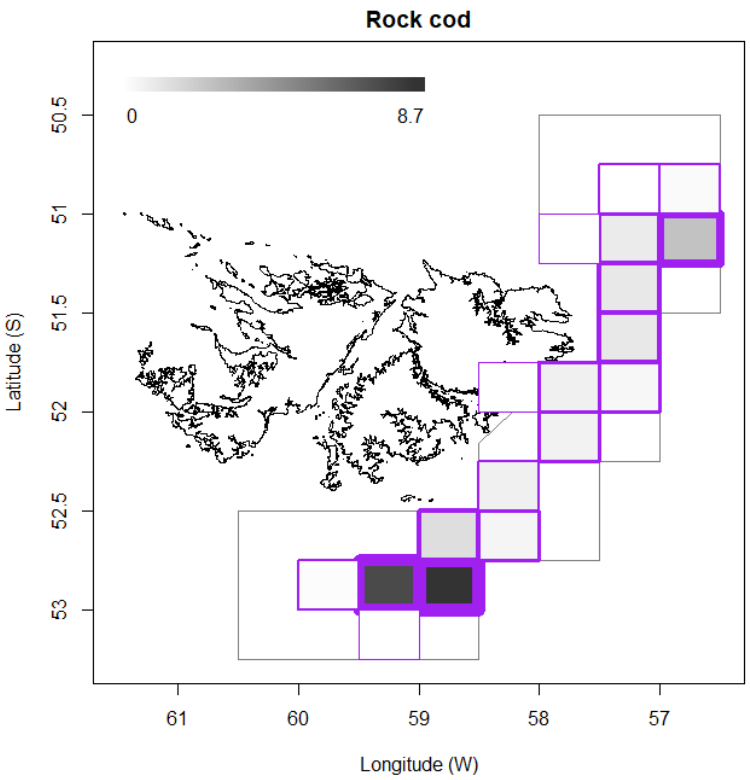
Rock cod
0
8.7
Latitude (S)
50.5
51
51.5
52
52.5
53
61
60
59
58
57
Longitude (W)

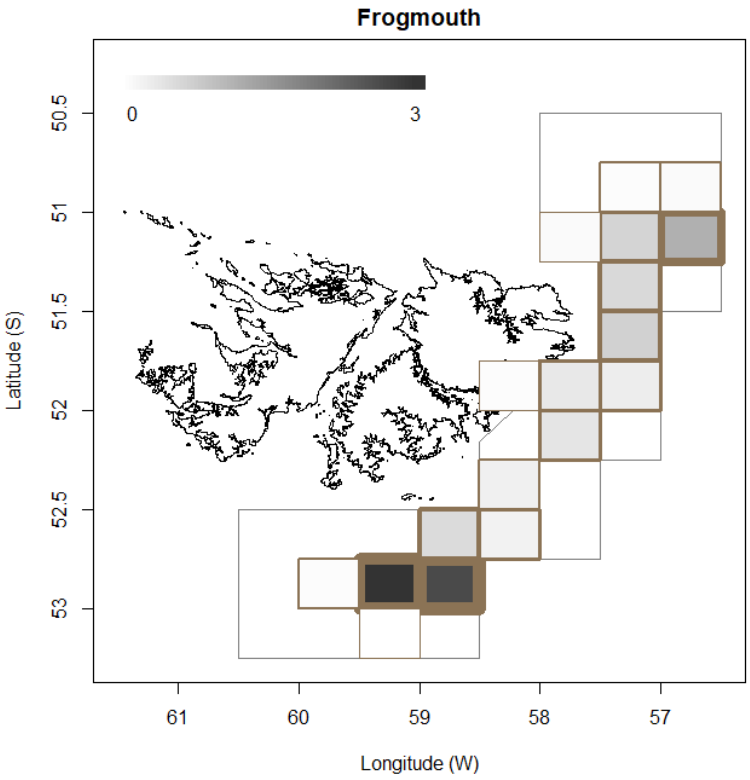

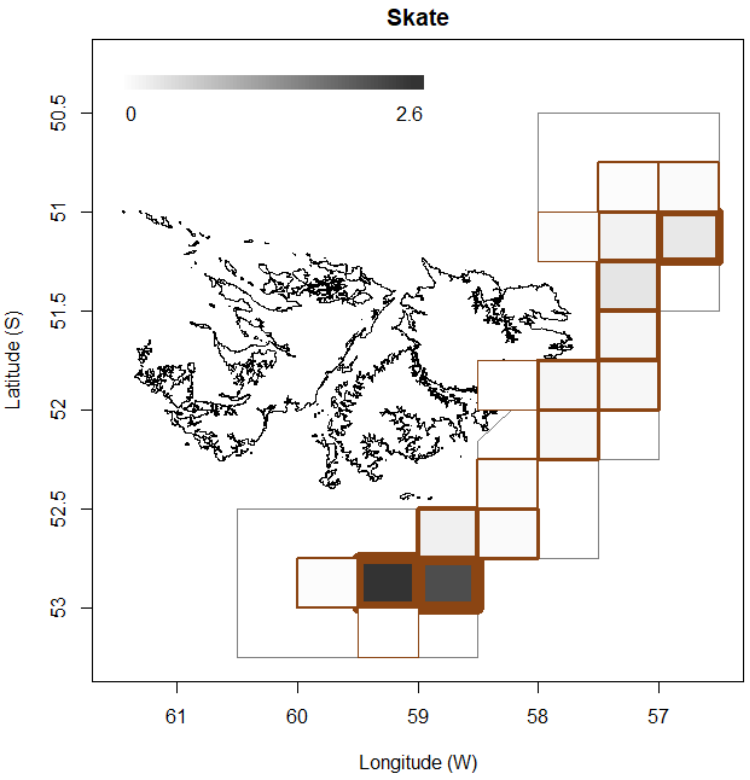

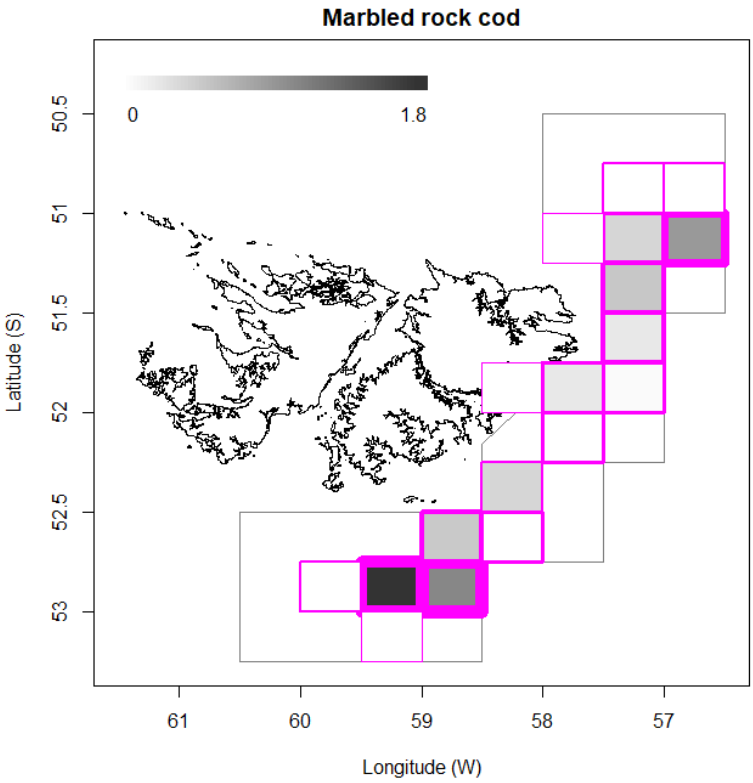

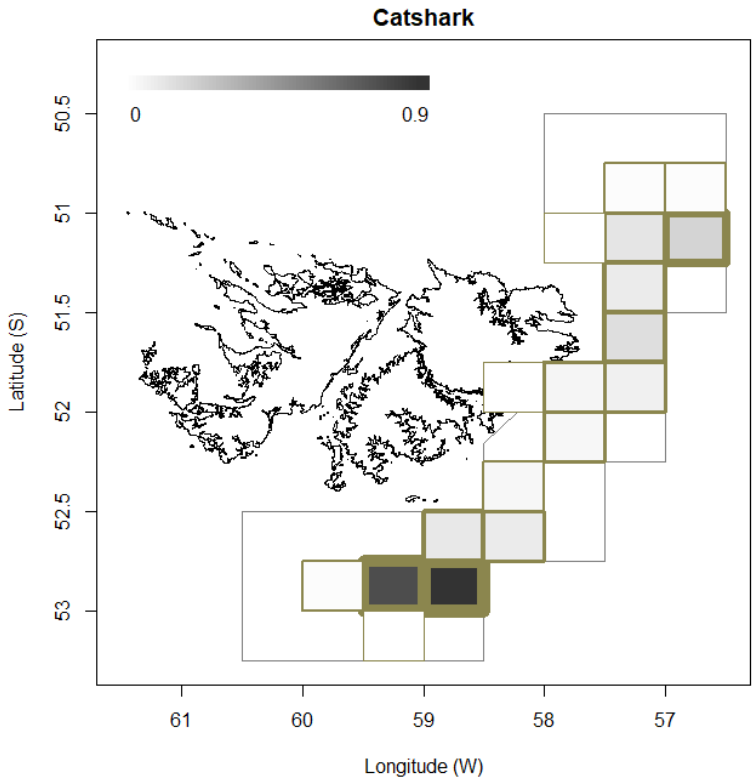

After scallops with 80.5 tonnes from 377 vessel-days (catch reports), highest aggregate bycatches in second season 2023 were common hake *Merluccius hubbsi* with 66.3 tonnes from 377 vessel-days, jellyfish Medusae (51.8 t, 283 v-days), common rock cod *Patagonotothen ramsayi* (26.3 t, 420 v-days), frogmouth *Cottoperca gobio* (11.0 t, 396 v-days), skates

Rajiformes (6.5 t, 332 v-days), marbled rock cod *Patagonotothen tessellata* (6.1 t, 134 v-days), and catshark *Schroederichthys bivius* (2.5 t, 239 v-days). Relative distributions by grid of these bycatches are shown in Figure 12; the complete list of all catches by species is in Table A1.

Trawl area coverage

The impact of bottom trawling on seafloor habitat has been a matter of concern in commercial fisheries (Kaiser et al. 2002; 2006), whereby the potential severity of impact relates to spatial and temporal extents of trawling (Piet and Hintzen 2012, Gerritsen et al. 2013), as well as the type of trawl gear (Rijnsdorp et al. 2020). For the *D. gahi* fishery, available catch, effort, and positional data are used to summarize the estimated 'ground' area coverage[c] occupied during the season of trawling.

The procedure for summarizing trawl area coverage is described in the Appendix of the second season 2019 report (Winter 2019). In second season 2023 50% of total *D. gahi* catch was taken from 2.1% of the total area of the Loligo Box, corresponding approximately[d] to the aggregate of grounds trawled ≥5.1 times. 90% of total *D. gahi* catch was taken from 8.1% of the total area of the Loligo Box, corresponding approximately to the aggregate of grounds trawled ≥2.2 times. 100% of total *D. gahi* catch over the season was taken from 11.8% of the total area of the Loligo Box, obviously corresponding to the aggregate of all grounds trawled at least once (Figure 13 - left). The 11.8% total trawl area coverage is just above the median of the eleven seasons that have been given this analysis so far. Averaged by 5 × 5 km grid (Figure 13 - right), 1 grid (out of 1383) had coverage >9 (that is to say, every patch of ground within that 5 × 5 km was on average trawled over 9 times or more). Fourteen grids had coverage of 5 or more, and 68 grids had coverage of 2 or more.

Among the eleven seasons given trawl area coverage analysis, all five seasons with above-median CPUE (total *D. gahi* catch divided by total vessel-days) had below-median cumulative area proportion trawled (Figure 14), a statistically significant contrast by permutation test ($p < 0.004$). The contrast suggests a change of state whereby seasons with less abundant catches trawl over wider areas, and vice-versa, although the relationship is not definitive enough for a parametric model (e.g., GLM or GAM).

[c] Appropriate spatial scale for calculating area coverage is a matter of some debate (Amoroso et al. 2018, Kroodsma et al. 2018). Given the comparatively small area of the Loligo Box, a high resolution of 5 km × 5 km was used for these calculations.

[d] However, not exactly. There is an expected strong correlation between the density of *D. gahi* catch taken from area units and how often these area units were trawled, but the correlation is not perfectly monotonic.

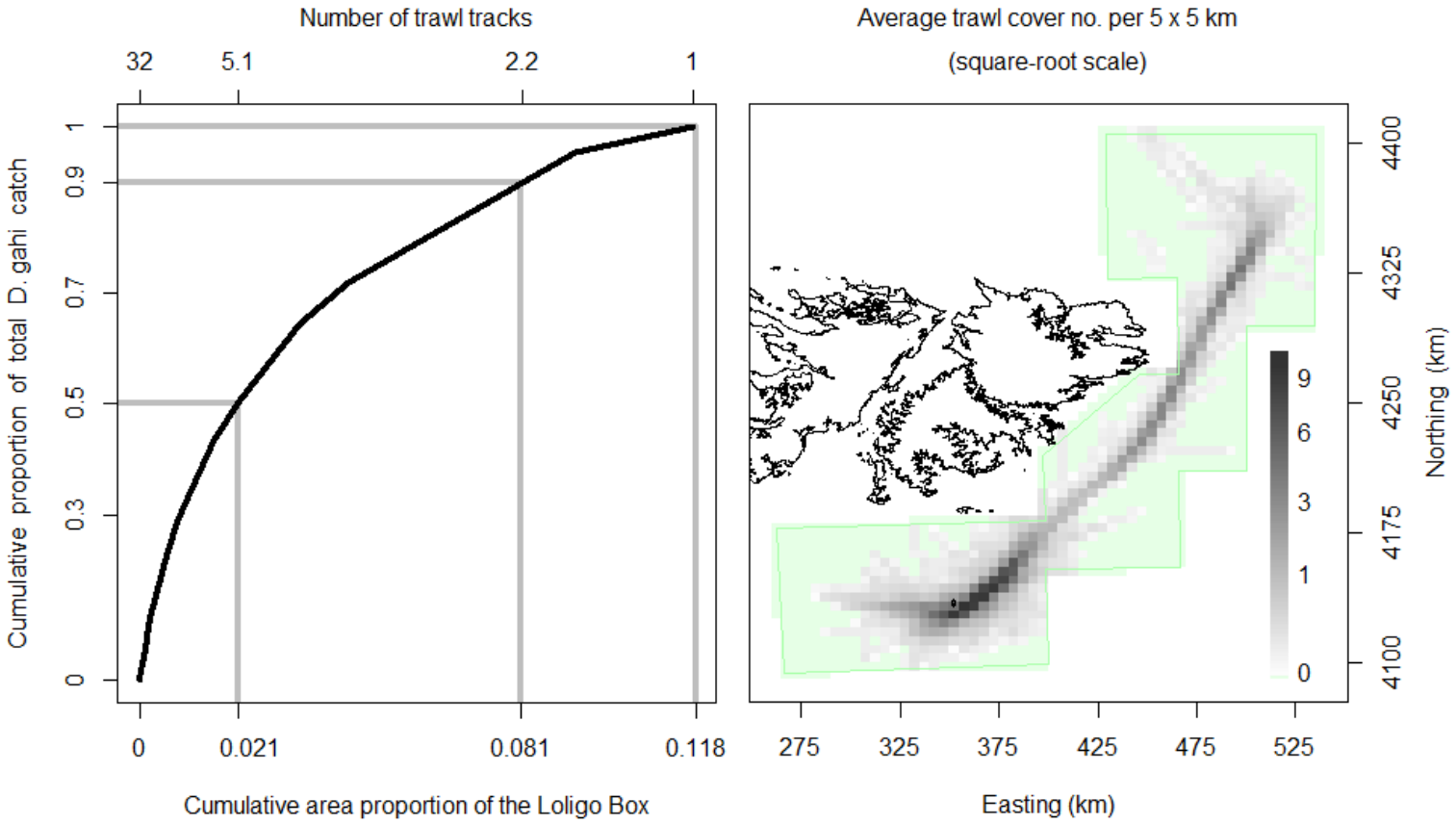

Figure 13. Left: cumulative *D. gahi* catch of 2nd season 2023, vs. cumulative area proportion of the Loligo Box the catch was taken from. The maximum number of times that any single area unit was trawled was 32, and catch cumulation by reverse density corresponded approximately to the trawl multiples shown on the top x-axis. Right: trawl cover averaged by 5 × 5 km grid; green area represents zero trawling.

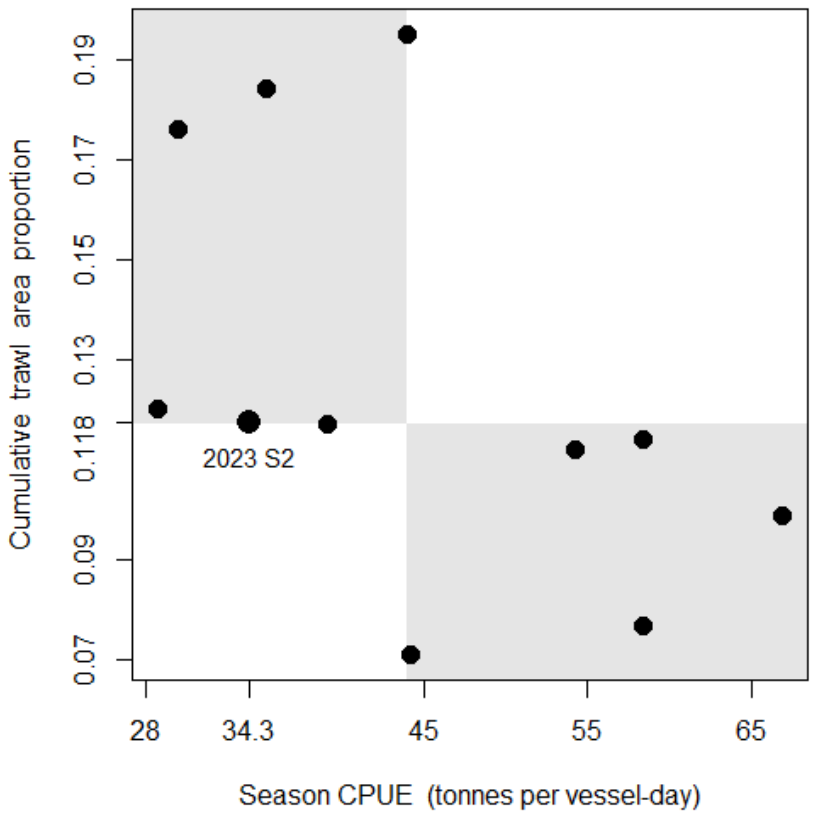

Figure 14. Season CPUEs vs. cumulative trawl area proportions. Opposite median brackets are grey under-shaded. The current season is marked.

References

Agnew, D.J., Baranowski, R., Beddington, J.R., des Clers, S., Nolan, C.P. 1998. Approaches to assessing stocks of *Loligo gahi* around the Falkland Islands. Fisheries Research 35: 155-169.

Agnew, D. J., Beddington, J. R., and Hill, S. 2002. The potential use of environmental information to manage squid stocks. Canadian Journal of Fisheries and Aquatic Sciences, 59: 1851-1857.

Akaike, H. 1973. Information theory and an extension of the maximum likelihood principle. 2nd International Symposium on Information Theory: 267-281.

Amoroso, R.O., Parma, A.M., Pitcher, C.R., McConnaughey, R.A., Jennings, S. 2018. Comment on "Tracking the global footprint of fisheries". Science 361: eaat6713.

Amukwaya, A. 2023. Observer Report 1372. Technical Document, FIG Fisheries Department. 23 p.

Arkhipkin, A. 1993. Statolith microstructure and maximum age of *Loligo gahi* (Myopsida: Loliginidae) on the Patagonian Shelf. Journal of the Marine Biological Association of the UK 73: 979-982.

Arkhipkin, A.I., Middleton, D.A.J. 2002. Sexual segregation in ontogenetic migrations by the squid *Loligo gahi* around the Falkland Islands. Bulletin of Marine Science 71: 109-127.

Arkhipkin, A.I., Middleton, D.A.J., Barton, J. 2008. Management and conservation of a short-lived fishery resource: *Loligo gahi* around the Falkland Islands. American Fisheries Society Symposium 49: 1243-1252.

Arkhipkin, A.I., Hendrickson, L.C., Payá, I., Pierce, G.J., Roa-Ureta, R.H., Robin, J.-P., Winter, A. 2021. Stock assessment and management of cephalopods: advances and challenges for short-lived fishery resources. ICES Journal of Marine Science 78: 714-730.

Barton, J. 2002. Fisheries and fisheries management in Falkland Islands Conservation Zones. Aquatic Conservation: Marine and Freshwater Ecosystems 12: 127-135.

Brooks, S.P., Gelman, A. 1998. General methods for monitoring convergence of iterative simulations. Journal of computational and graphical statistics 7: 434-455.

Carlson, J.E. 2014. A generalization of Pythagoras's theorem and application to explanations of variance contributions in linear models. Research Report No. RR-14-18, Princeton, NJ: Educational Testing Service. 17 p.

Chemshirova, I., Hoyer, P., Nicholls, R., Winter, A. 2023. Falkland calamari (*Doryteuthis gahi*) 2nd pre-season 2023 stock assessment survey. Technical Document, Falkland Islands Fisheries Department. 20 p.

DeLury, D.B. 1947. On the estimation of biological populations. Biometrics 3: 145-167.

FIFD. 2004. Fishery Report, *Loligo gahi*, Second Season 2004. Fishing statistics, biological trends, and stock assessment. Technical Document, Falkland Islands Fisheries Department. 15 p.

Gamerman, D., Lopes, H.F. 2006. Markov Chain Monte Carlo. Stochastic simulation for Bayesian inference. 2nd edition. Chapman & Hall/CRC.

Gerritsen, H.D., Minto, C., Lordan, C. 2013. How much of the seabed is impacted by mobile fishing gear? Absolute estimates from Vessel Monitoring System (VMS) point data. ICES Journal of Marine Science 70: 523-531.

Hoenig, J. M. 1982. A compilation of mortality and longevity estimates for fish, molluscs, and cetaceans, with a bibliography of comparative life history studies. University of Rhode Island, Graduate School of Oceanography, Technical Report, 82-2. 14 p.

Hoenig, J.M. 1983. Empirical use of longevity data to estimate mortality rates. Fishery Bulletin 82: 898-903

Kaiser, M.J., Collie, J.S., Hall, S.J., Jennings, S., Poiner, I.R. 2002. Modification of marine habitats by trawling activities: prognosis and solutions. Fish and Fisheries 3: 114-136.

Kaiser, M.J., Clarke, K.R., Hinz, H., Austen, M.C.V., Somerfield, P.J., Karakassis, I. 2006. Global analysis of response and recovery of benthic biota to fishing. Marine Ecology Progress Series 311: 1-14.

Kroodsma, D.A., Mayorga, J., Hochberg, T., Miller, N.A., Boerder, K., Ferretti, F., Wilson, A., Bergman, B., White, T.D., Block, B.A., Woods, P., Sullivan, B., Costello, C., Worm, B. 2018. Response to Comment on "Tracking the global footprint of fisheries". Science 361: eaat7789.

Lipiński, M. R. 1979. Universal maturity scale for the commercially important squids (Cephalopoda: Teuthoidea). The results of maturity classification of *Illex illecebrosus* (Le Sueur 1821) population for years 1973-1977. ICNAF Research Document 79/11/38, 40 p.

MacCall, A.D. 2009. Depletion-corrected average catch: a simple formula for estimating sustainable yields in data-poor situations. ICES Journal of Marine Science 66: 2267-2271.

Magnusson, A., Punt, A., Hilborn, R. 2013. Measuring uncertainty in fisheries stock assessment: the delta method, bootstrap, and MCMC. Fish and Fisheries 14: 325-342.

Nash, J.C., Varadhan, R. 2011. optimx: A replacement and extension of the optim() function. R package version 2011-2.27. http://CRAN.R-project.org/package=optimx

Nicholls, R. 2023. Observer Report 1369. Technical Document, FIG Fisheries Department. 26 p.

Patterson, K.R. 1988. Life history of Patagonian squid *Loligo gahi* and growth parameter estimates using least-squares fits to linear and von Bertalanffy models. Marine Ecology Progress Series 47: 65-74.

Payá, I. 2006. Fishery Report. *Loligo gahi*, Second Season 2006. Fishery statistics, biological trends, stock assessment and risk analysis. Technical Document, Falkland Islands Fisheries Dept. 40 p.

Payá, I. 2010. Fishery Report. *Loligo gahi*, Second Season 2009. Fishery statistics, biological trends, stock assessment and risk analysis. Technical Document, Falkland Islands Fisheries Dept. 54 p.

Pierce, G.J., Guerra, A. 1994. Stock assessment methods used for cephalopod fisheries. Fisheries Research 21: 255-285.

Piet, G.J., Hintzen, N.T. 2012. Indicators of fishing pressure and seafloor integrity. ICES Journal of Marine Science 69: 1850-1858.

Plet-Hansen, K.S., Larsen, E., Mortensen, L.O., Nielsen, J.R., Ulrich, C. 2018. Unravelling the scientific potential of high-resolution fishery data. Aquatic Living Resources 31:24.

Punt, A.E., Hilborn, R. 1997. Fisheries stock assessment and decision analysis: the Bayesian approach. Reviews in Fish Biology and Fisheries 7: 35-63.

Rijnsdorp, A.D., Hiddink, J.G., van Denderen, P.D., Hintzen, N.T., Eigaard, O.R., Valanko, S., Bastardie, F., Bolam, S.G., Boulcott, P., Egekvist, J., Garcia, C., van Hoey, G., Jonsson, P., Laffargue, P., Nielsen, J.R., Piet, G.J., Sköld, M., van Kooten, T. 2020. Different bottom trawl fisheries have a differential impact on the status of the North Sea seafloor habitats. ICES Journal of Marine Science 77: 1772-1786.

Roa-Ureta, R. 2012. Modelling in-season pulses of recruitment and hyperstability-hyperdepletion in the *Loligo gahi* fishery around the Falkland Islands with generalized depletion models. ICES Journal of Marine Science 69: 1403-1415.

Roa-Ureta, R., Arkhipkin, A.I. 2007. Short-term stock assessment of *Loligo gahi* at the Falkland Islands: sequential use of stochastic biomass projection and stock depletion models. ICES Journal of Marine Science 64: 3-17.

Rosenberg, A.A., Kirkwood, G.P., Crombie, J.A., Beddington, J.R. 1990. The assessment of stocks of annual squid species. Fisheries Research 8: 335-350.

Shaw, P.W., Arkhipkin, A.I., Adcock, G.J., Burnett, W.J., Carvalho, G.R., Scherbich, J.N., Villegas, P.A. 2004. DNA markers indicate that distinct spawning cohorts and aggregations of Patagonian squid, *Loligo gahi*, do not represent genetically discrete subpopulations. Marine Biology, 144: 961-970.

Swartzman, G., Huang, C., Kaluzny, S. 1992. Spatial analysis of Bering Sea groundfish survey data using generalized additive models. Canadian Journal of Fisheries and Aquatic Sciences 49: 1366-1378.

Winter, A. 2019. Stock assessment – Falkland calamari *Doryteuthis gahi* 2nd season 2019. Technical Document, Falkland Islands Fisheries Department. 36 p.

Winter, A., Skeljo, F. 2022. Stock assessment – Falkland calamari *Doryteuthis gahi* 1st season 2022. Technical Document, Falkland Islands Fisheries Department. 30 p.

Winter, A., Skeljo, F. 2022. Stock assessment – Falkland calamari *Doryteuthis gahi* 2nd season 2022. Technical Document, Falkland Islands Fisheries Department. 33 p.

Winter, A., Arkhipkin, A. 2015. Environmental impacts on recruitment migrations of Patagonian longfin squid (*Doryteuthis gahi*) in the Falkland Islands with reference to stock assessment. Fisheries Research 172: 85-95.

Appendix
***Doryteuthis gahi* individual weights**

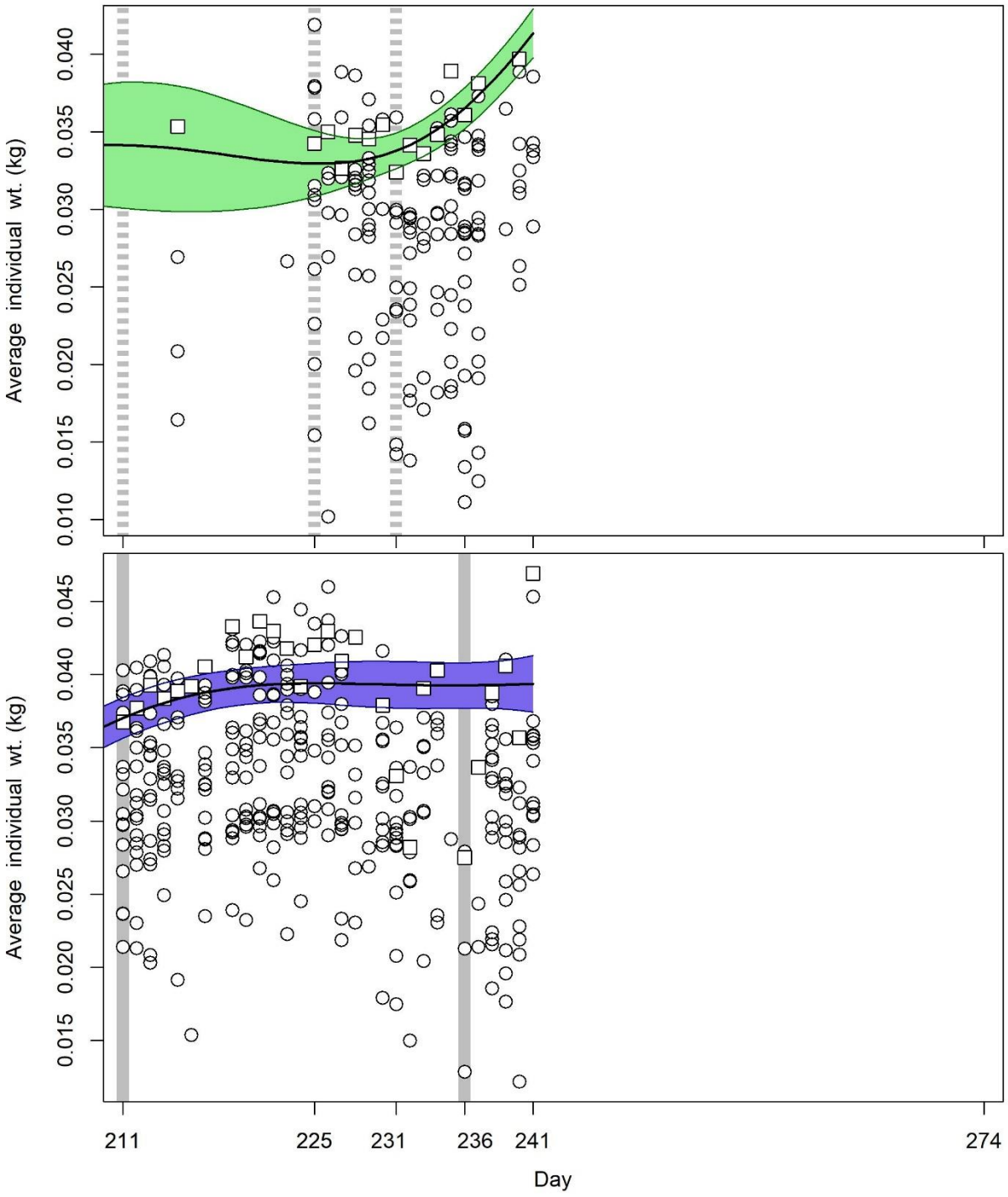

Figure A1. North (top) and south (bottom) sub-area daily average individual *D. gahi* weights from commercial size categories per vessel (circles) and observer measurements (squares). GAMs of the daily trends ± 95% confidence interval (centre lines and colour under-shading).

To smooth fluctuations, GAM trends were calculated of daily average individual weights. North and south sub-areas were calculated separately. For continuity, GAMs were calculated

using all pre-season survey and in-season data contiguously. North and south GAMs were first calculated separately on the commercial and observer data. As full observer coverage in the *D. gahi* fishery has now become standard, observer data GAMs were taken as the baseline trends, augmented by the margin by which commercial data are more frequent than observer data (if at all). For example, this season had 452 commercial fishing days (Table 1), and 431 observer days (FIG + contract observers). The final GAM trend was therefore calculated as:

$$\mathrm{GAM_{Wt}} = \mathrm{Obs\ GAM_{Wt}} - \left(1 - \mathrm{pmin}\left(1, \frac{431}{452}\right)\right) \times \mathrm{mean}(\mathrm{Obs\ GAM_{Wt}} - \mathrm{Comm\ GAM_{Wt}})$$

As before, inclusion of both GAMs effected that the greater day-to-day consistency of the commercial data trends, and the greater point value accuracy of the observer data, are represented in the calculations. GAM plots of the north and south sub-areas are in Figure A1.

Prior estimates and CV

The pre-season survey had estimated *D. gahi* biomass of 19,859 tonnes (Chemshirova et al. 2023). Hierarchical bootstrapping of the inverse distance weighting algorithm obtained a coefficient of variation (CV) equal to 15.1% of the survey biomass distribution. From modelled survey catchability, Payá (2010) had estimated average net escapement of up to 22%, which was added to the CV:

$$19{,}859 \pm (.151 + .22) = 19{,}859 \pm 37.1\% = 19{,}859 \pm 7{,}367 \text{ t} \qquad \textbf{(A1)}$$

The 22% escapement was added as a linear increase in the variability, but was not used to reduce the total estimate, because squid that escape one trawl are likely to be part of the biomass concentration that is available to the next trawl.

D. gahi numbers from the survey were estimated as the survey biomasses divided by the GAM-predicted individual weight average for the survey: 0.0365 kg. The average coefficient of variation (CV) of the GAM over the duration of the pre-season survey was 2.7%, and CV of the length-weight conversion relationship (Equation **7**) was 10.5%. Joining these sources of variation with the pre-season survey biomass estimates and individual weight averages (above) gave estimated *D. gahi* numbers at survey end (day 208) of:

$$\begin{aligned} {}_{\text{prior}}\mathrm{N}_{\text{day 208}} &= \frac{19{,}859 \times 1000}{0.0365} \pm \sqrt{37.1\%^2 + 2.7\%^2 + 10.5\%^2} \\ &= 0.545 \times 10^9 \pm 38.6\% \end{aligned} \qquad \textbf{(A2)}$$

The combined catchability coefficient (q) prior was taken on day 211, the first day of the season, when 16 vessels fished in the south sub-area and no vessels fished in the north sub-area (16 total; Figure 3). Abundance on day 211 was discounted for natural mortality over the 3 days since the end of the survey:

$${}_{\text{prior}}\mathrm{N}_{\text{day 211}} = {}_{\text{prior}}\mathrm{N}_{\text{day 208}} \times e^{-M\cdot(211-208)} - \mathrm{CNMD}_{\text{day 211}} = 0.523 \times 10^9 \qquad \textbf{(A3)}$$

where $\mathrm{CNMD}_{\text{day 211}} = 0$ as no catches intervened between the end of the survey and the start of commercial season. Thus:

$$_{prior}q = C(N)_{day\ 211} / (_{prior}N_{day\ 211} \times E_{day\ 211})$$

$$= (C(B)_{day\ 211} / Wt_{day\ 211}) / (_{prior}N_{day\ 211} \times E_{day\ 211})$$

$$= (1{,}054.3\ t / 0.0389\ kg) / (0.523 \times 10^{9} \times 16\ vessel\text{-}days)$$

$$= 3.238 \times 10^{-3}\ vessels^{-1}$$ [e] **(A4)**

$SD_{prior\ q}$ (Equation **4**) was calculated as $_{prior}q$ multiplied by its CV. $CV_{prior\ q}$ was calculated as the sum of variability in $_{prior}N_{day\ 208}$ (Equation **A2**) plus variability in the catches of vessels on start day 211, plus variability of the natural mortality (see Appendix section Natural mortality).

$$CV_{prior\ q} = \sqrt{38.6\%^2 + \left(\frac{SD\left(C(B)_{vessels\ day\ 211}\right)}{mean\left(C(B)_{vessels\ day\ 211}\right)}\right)^2 + (1 - (1 - CV_M)^{(211\ -\ mid\_survey)})^2}$$

$$= \sqrt{38.6\%^2 + 24.4\%^2 + 99.9\%^2} = 109.9\%$$

$$SD_{prior\ q} = {}_{prior}q \times CV_{prior\ q} = 3.557 \times 10^{-3}\ vessels^{-1}$$ **(A5)**

Depletion model estimates and CV

For the south sub-area, the equivalent of Equation **2** with two N_{day} was optimized on the difference between predicted and actual catches (Equation **3**), resulting in parameters values:

$$_{depletion}N1_{S\ day\ 211} = 0.549 \times 10^{9}; \quad _{depletion}N2_{S\ day\ 236} = 0.043 \times 10^{9}$$

$$_{depletion}q_{S} = 3.137 \times 10^{-3}$$ [f] **(A6-S)**

The normalized root-mean-square deviation of predicted vs. actual catches was calculated as the CV of the model:

$$CV_{rmsd\ S} = \frac{\sqrt{\sum_{i=1}^{n}\left({}_{predicted}C(N)_{S\ day\ i} - {}_{actual}C(N)_{S\ day\ i}\right)^2 / n}}{mean\left({}_{actual}C(N)_{S\ day\ i}\right)}$$

$$= 4.004 \times 10^{6} / 10.134 \times 10^{6} = 39.5\%$$ **(A7-S)**

$CV_{rmsd\ S}$ was added to the variability of the GAM-predicted individual weight averages for the season (Figure A1-S); equal to a CV of 1.84% south. CVs of the depletion were then calculated as the sum:

$$CV_{depletion\ S} = \sqrt{CV_{rmsd\ S}^{\ 2} + CV_{GAM\ Wt\ S}^{\ 2}} = \sqrt{39.5\%^2 + 1.84\%^2}$$

$$= 39.6\%$$ **(A8-S)**

[e] On Figure 6-left and Figure 8-left.
[f] On Figure 6-left.

For the north sub-area, the Equation **2** equivalent with three N_{day} was optimized on the difference between predicted and actual catches (Equation **3**), resulting in parameter values:

$$_{depletion}N1_{N\ day\ 211} = 0.049 \times 10^9; \quad _{depletion}N2_{N\ day\ 225} = 0.096 \times 10^9$$
$$_{depletion}N3_{N\ day\ 231} = 0.029 \times 10^9$$
$$_{depletion}q_N = 7.501 \times 10^{-3}\ ^g \qquad \textbf{(A6-N)}$$

Root-mean-square deviation of predicted vs. actual catches was calculated as the CV of the model:

$$CV_{rmsd\ N} = \frac{\sqrt{\sum_{i=1}^{n}\left({}_{predicted}C(N)_{N\ day\ i} - {}_{actual}C(N)_{N\ day\ i}\right)^2 / n}}{mean\left({}_{actual}C(N)_{N\ day\ i}\right)}$$

$$= 1.319 \times 10^6 / 3.113 \times 10^6 = 42.4\% \qquad \textbf{(A7-N)}$$

$CV_{rmsd\ N}$ was added to the variability of the GAM-predicted individual weight averages for the season (Figure A1-N); equal to a CV of 2.37% north. CVs of the depletion were then calculated as the sum:

$$CV_{depletion\ N} = \sqrt{CV_{rmsd\ N}{}^2 + CV_{GAMWt\ N}{}^2} = \sqrt{42.4\%^2 + 2.37\%^2}$$
$$= 42.5\% \qquad \textbf{(A8-N)}$$

Combined Bayesian models

For the south sub-area, joint optimization of Equations **3** and **4** resulted in parameters values:

$$_{Bayesian}N1_{S\ day\ 211} = 1.547 \times 10^9; \quad _{Bayesian}N2_{S\ day\ 236} = 0.043 \times 10^9$$
$$_{Bayesian}q_S = 3.137 \times 10^{-3}\ ^h \qquad \textbf{(A9-S)}$$

These parameters produced the fit between predicted catches and actual catches shown in Figure A2-S.

For the north sub-area, joint optimization of Equations **3** and **4** resulted in parameters values:

$$_{Bayesian}N1_{N\ day\ 211} = 0.087 \times 10^9; \quad _{Bayesian}N2_{N\ day\ 225} = 0.155 \times 10^9$$
$$_{Bayesian}N3_{N\ day\ 231} = 0.006 \times 10^9$$
$$_{Bayesian}q_N = 4.254 \times 10^{-3}\ ^i \qquad \textbf{(A9-N)}$$

These parameters produced the fit between predicted catches and actual catches shown in Figure A2-N.

[g] On Figure 8-left.
[h] On Figure 6-left.
[i] On Figure 8-left.

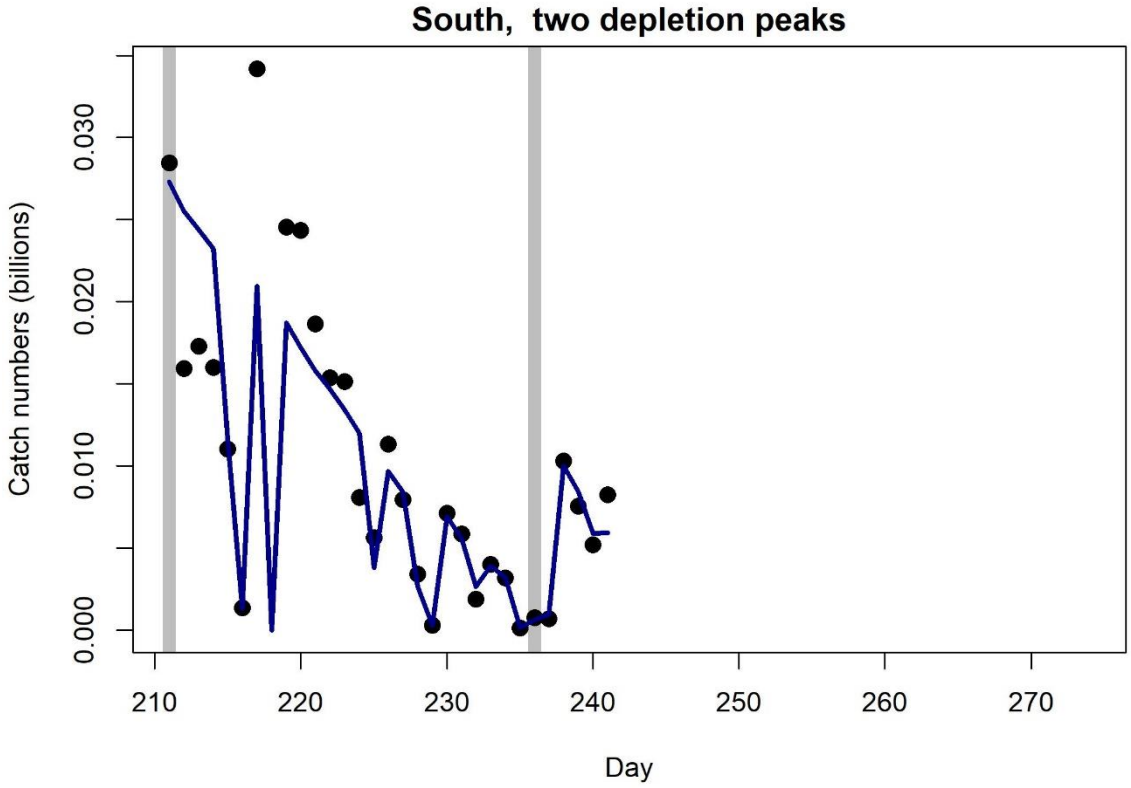

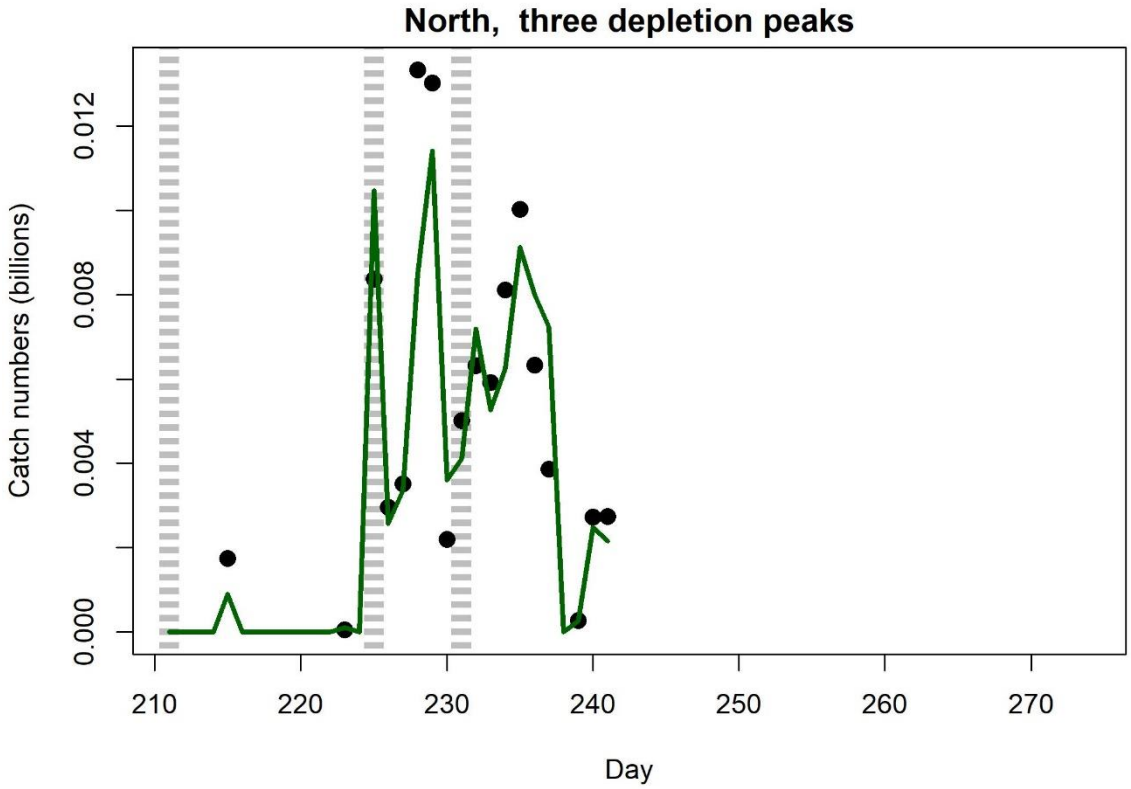

Figure A2-S [top]. Daily catch numbers estimated from actual catch (black points) and predicted from the depletion model (purple line) in the south sub-area.

Figure A2-N [bottom]. Daily catch numbers estimated from actual catch (black points) and predicted from the depletion model (green line) in the north sub-area.

Natural mortality

Natural mortality is parameterized as a constant instantaneous rate M = 0.0133 day^{-1} (Roa-Ureta and Arkhipkin 2007), based on Hoenig's (1983) log mortality vs. log maximum age regression, applied to an estimated maximum age of 352 days for *D. gahi*:

$$\log(M) = 1.44 - 0.982 \times \log(age_{max})$$

$$M = \exp(1.44 - 0.982 \times \log(352))$$

$$= 0.0133 \quad \textbf{(A10)}$$

Hoenig (1983) derived Equation **A10** from the regression of 134 stocks among 79 species of fish, molluscs, and cetaceans. Hoenig's regression obtained $R^2 = 0.82$, but a corresponding coefficient of variation (CV) was not published. The CV is estimated by re-computing the regression from original data in Hoenig (1982)[j], extracting the standard error (σ), and calculating the CV from the equation:

$$CV = (\exp(\sigma^2) - 1)^{½} \quad \text{(MacCall 2009)}$$

which gave

$$CV_M = (\exp(0.472^2) - 1)^{½} = 49.96\% \quad \textbf{(A11)}$$

MacCall (2009) suggested that CV_M should be assumed a minimum of 0.5, effectively equivalent to Equation **A11**.

CV_M was aggregated over the number of days between the midpoint of the survey and the commercial season start, rather than between the end of the survey and commercial season start, as the midpoint more accurately reflects how much time has elapsed since the fishing area on average was surveyed. The midpoint of the survey was calculated as the mean day weighted by the number of survey trawls taken per day:

$$\text{mid\_survey} = \frac{\Sigma\left(\text{day} \times N_{\text{survey trawls}}|_{\text{day}}\right)}{\Sigma\left(N_{\text{survey trawls}}|_{\text{day}}\right)} = 201^{k} \quad \textbf{(A12)}$$

CV_M was thus further indexed by $1 - (1 - CV_M)$ to ensure that the value could not decrease if CV_M was hypothetically > 100%:

$$1 - (1 - CV_M)^{(\text{commercial season start} - \text{mid\_survey})} \quad \textbf{(A13)}$$

Equation **A13** is included in Equation **A5**.

[j] Hoenig (1982) listed 130 rather than 134 stocks, but these 130 stocks obtained the same regression parameters of 1.44 and –0.982.

[k] In common nomenclature day 201 is July 20th.

Total catch by species

Table A1: Total reported catches and discard by taxon during first season 2023 X-license fishing, and number of catch reports (vessel-days) in which each taxon occurred. Does not include incidental catches of pinnipeds or seabirds.

Species Code	Species / Taxon	Catch Wt. (KG)	Discard Wt. (KG)	N Reports
LOL	*Doryteuthis gahi*	15513101	30165	452
SCA	*Zygochlamys patagonica*	80504	80375	377
HAK	*Merluccius hubbsi*	66331	7829	373
MED	Medusae sp.	51817	51817	283
PAR	*Patagonotothen ramsayi*	26309	26275	420
CGO	*Cottoperca gobio*	11037	11023	396
RAY	Rajiformes	6524	3577	332
PTE	*Patagonotothen tessellata*	6066	6066	134
DGH	*Schroederichthys bivius*	2511	2511	239
AST	Asteroidea	2399	2399	24
SAR	*Sprattus fuegensis*	1630	1624	106
LIM	*Lithodes murrayi*	1048	1048	75
TOO	*Dissostichus eleginoides*	789	780	209
OCT	Octopus spp.	781	781	88
UCH	*Strongylocentotus* spp.	576	576	41
ING	*Moroteuthis ingens*	524	524	86
LIT	*Lithodes turkayi*	485	485	31
MYX	Myxinidae	390	390	50
SPN	Porifera	373	373	7
BAC	*Salilota australis*	186	96	30
BLU	*Micromesistius australis*	157	157	20
GRV	Macrouridae	154	154	25
MUL	*Eleginops maclovinus*	99	99	26
ILL	*Illex argentinus*	61	61	15
DGS	*Squalus acanthias*	60	60	7
BUT	*Stromateus brasiliensis*	54	54	16
GRH	*Macrourus holotrachys*	33	33	2
MUN	*Grimothea gregaria*	32	32	9
KIN	*Genypterus blacodes*	28	28	10
GRF	*Coelorinchus fasciatus*	20	20	1
EEL	*Iluocoetes fimbriatus*	14	14	8
CHE	*Champsocephalus esox*	10	10	5
COT	*Cottunculus granulosus*	10	10	2
GRC	*Macrourus carinatus*	9	9	2
WHI	*Macruronus magellanicus*	8	8	3
RED	*Sebastes oculatus*	7	7	6
ALF	*Allothunnus fallai*	4	4	1
COP	*Congiopodus peruvianus*	3	3	2
NEM	*Psychrolutes marmoratus*	3	3	2
PAT	*Merluccius australis*	2	2	1
NOW	*Paranotothenia magellanica*	1	1	1
Total		15774150	229483	452